Coherent effects of multiple scattering: simulation and experimental studies

Igor Meglinski

University of Otago, New Zealand

E-mail: igor@physics.otago.ac.nz


New Zealand
Cape Reinga
Bay of Islands
Whangerei
Hauraki Gulf
Auckland
Coromandel Peninsula
Tasman Sea
Bay of Plenty
Hamilton
Tauranga
North Island
Rotorua
Raukumara Range
Tongariro
National Park
Gisborne
Hawke Bay
Napier
Wanganui
Hastings
Tasman Bay
Abel Tasman
National Park
Nelson
Wellington
Westport
Blenheim
Cook Strait
Greymouth
Kaikura
South Island
Franz Josef Glacier
Fox Glacier
Pegasus Bay
Christchurch
Southern Alps
Map © bugbog.com
Milford Sound
Otago Peninsula
South Pacific Ocean
Dunedin
Invercargill
Stewart Island

Medical Diagnostic

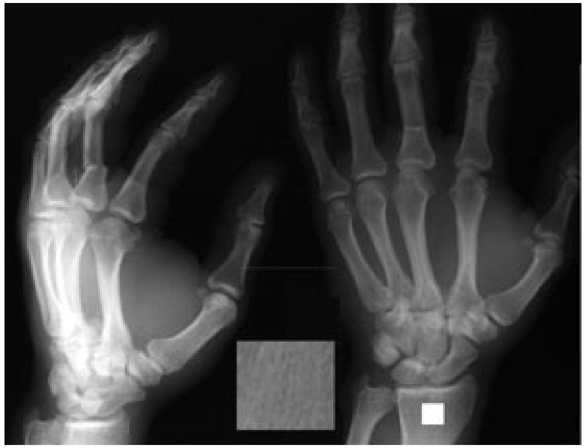
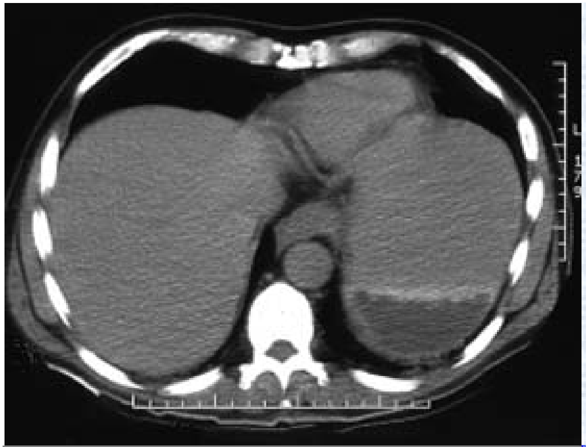
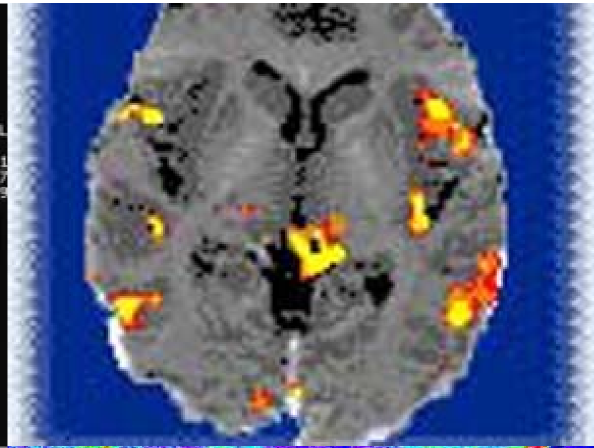



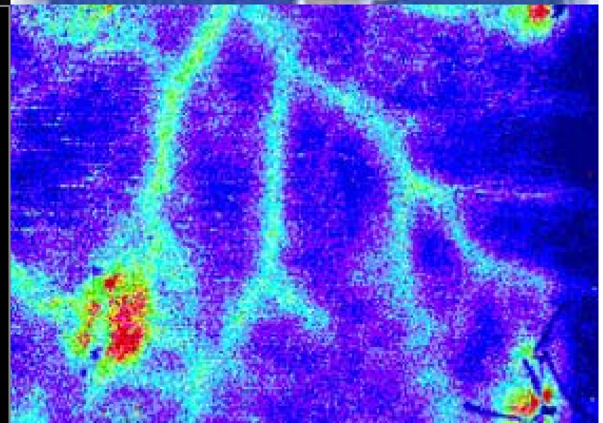
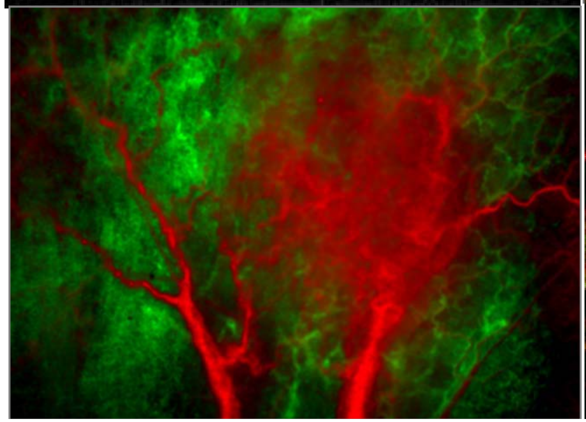
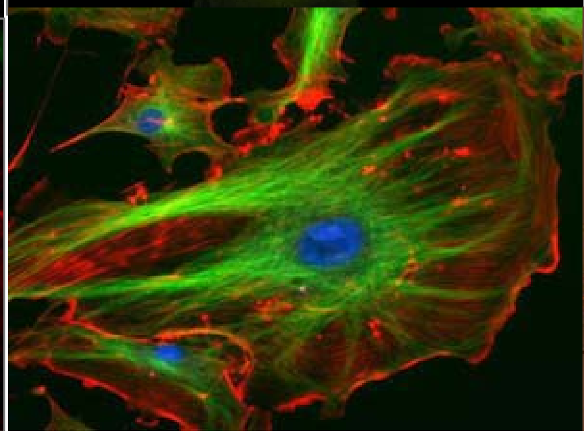
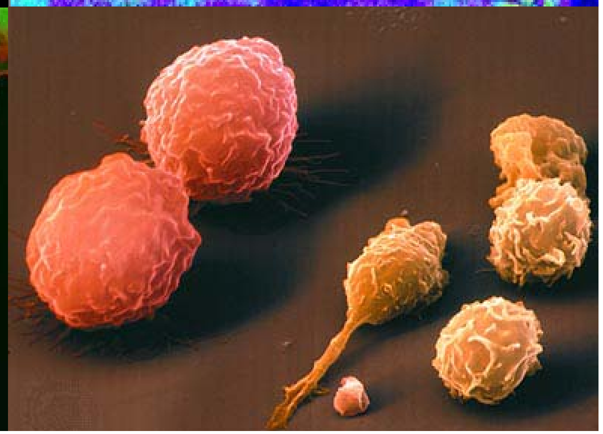

Bio-Photonics

The term Bio-Photonics denotes a combination of biology and photonics, with photonics being the science and technology of generation, manipulation, and detection of photons, quantum units of light. Photonics is related to electronics in that it is believed that photons will play a similar central role in future information technology as electrons do today.

Bio-photonics has therefore become the established general term for all techniques that deal with the interaction between biological items and photons. This refers to emission, detection, absorption, reflection, modification, and creation of radiation from bio-molecular, cells, tissues, organisms and biomaterials. Areas of application are life science, medicine, agriculture, and environmental science.

http://en.wikipedia.org/wiki/Biophotonics

Coherence

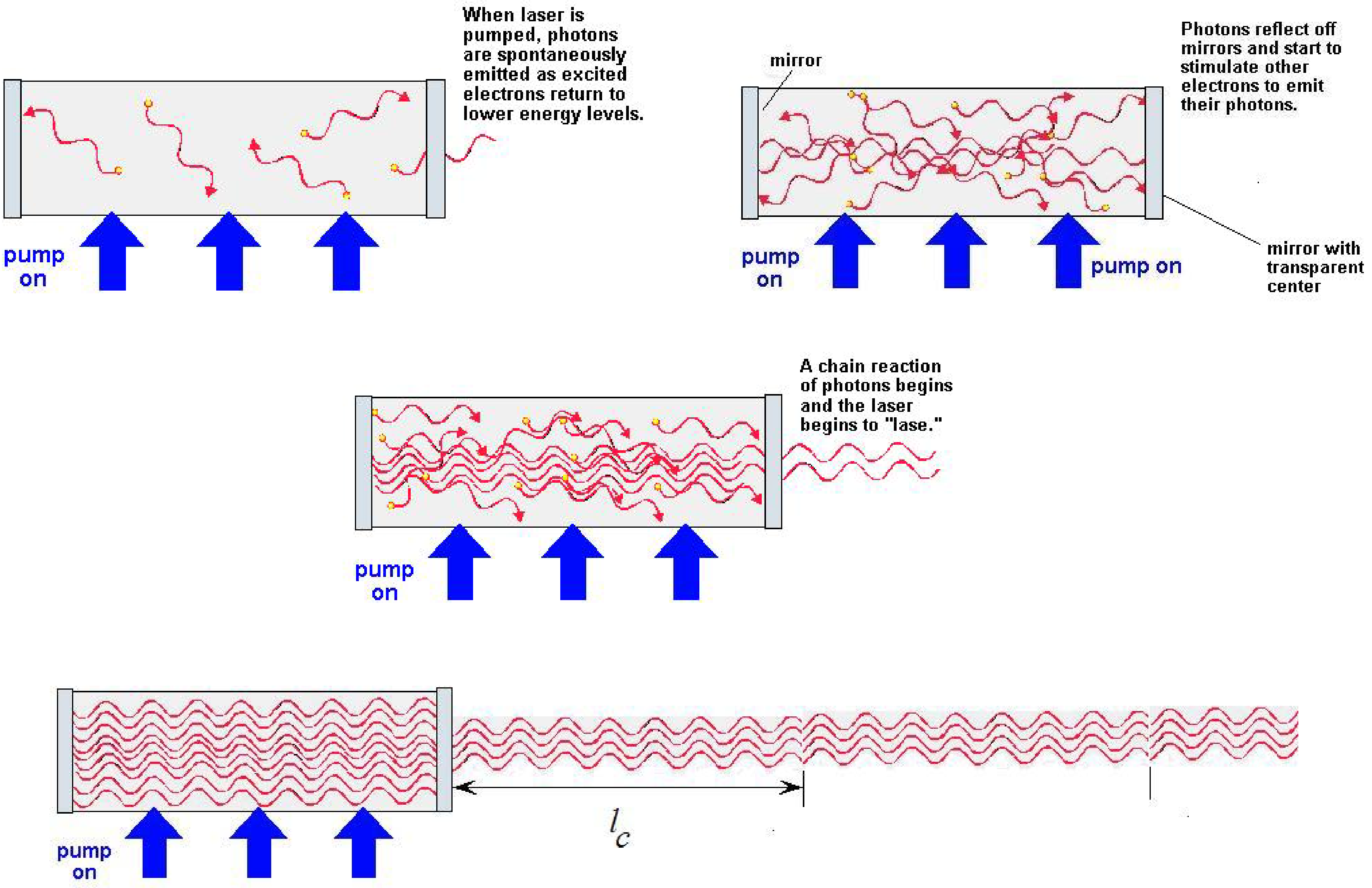

When laser is pumped, photons are spontaneously emitted as excited electrons return to lower energy levels.
pump on
mirror
Photons reflect off mirrors and start to stimulate other electrons to emit their photons.
pump on
pump on
mirror with transparent center
A chain reaction of photons begins and the laser begins to "lase."
pump on
l_c
pump on

Coherence

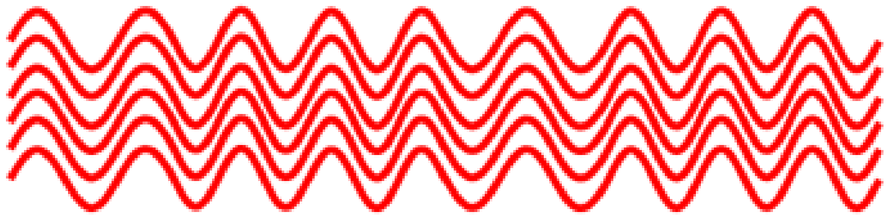

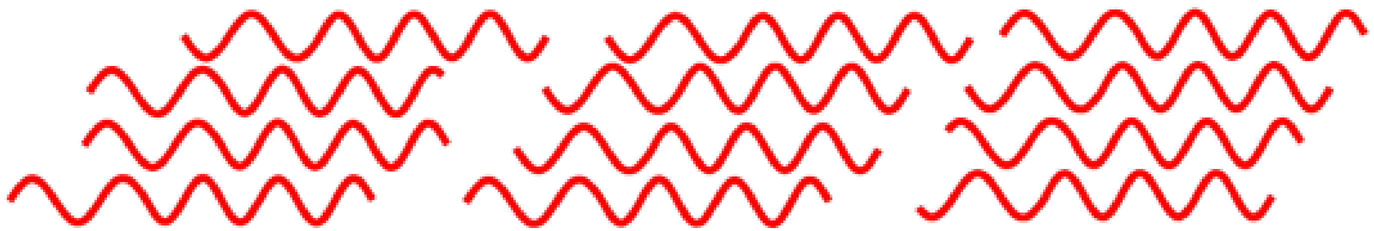

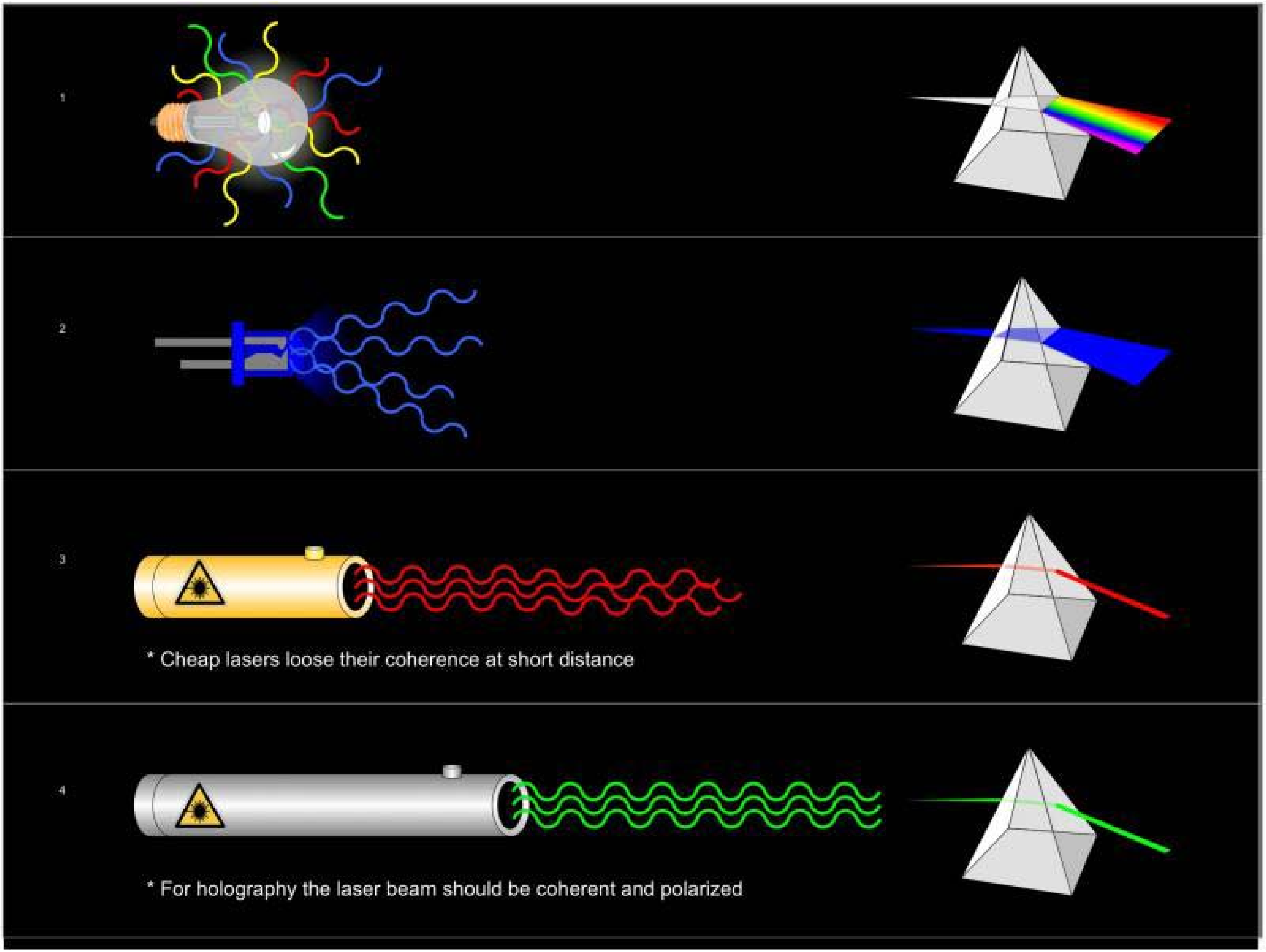
1
2
3
* Cheap lasers loose their coherence at short distance
4
* For holography the laser beam should be coherent and polarized

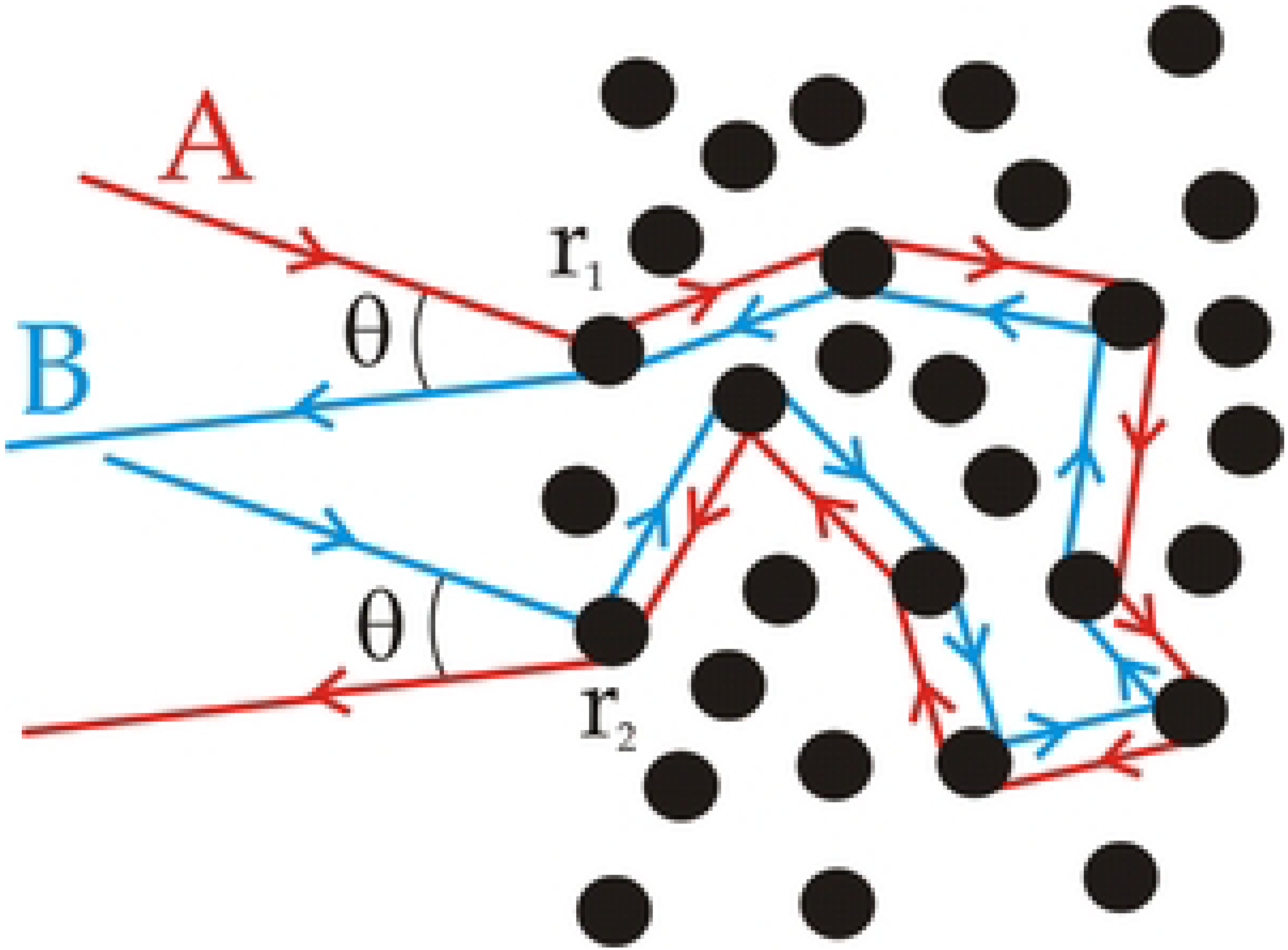
A
B
θ
θ
r_1
r_2

Enhancement of back-scattering

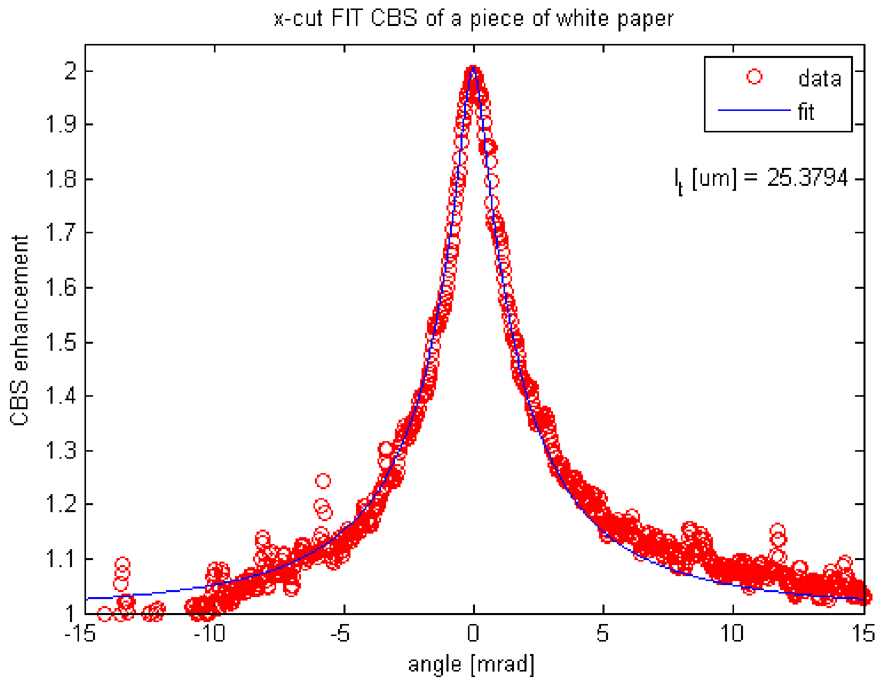

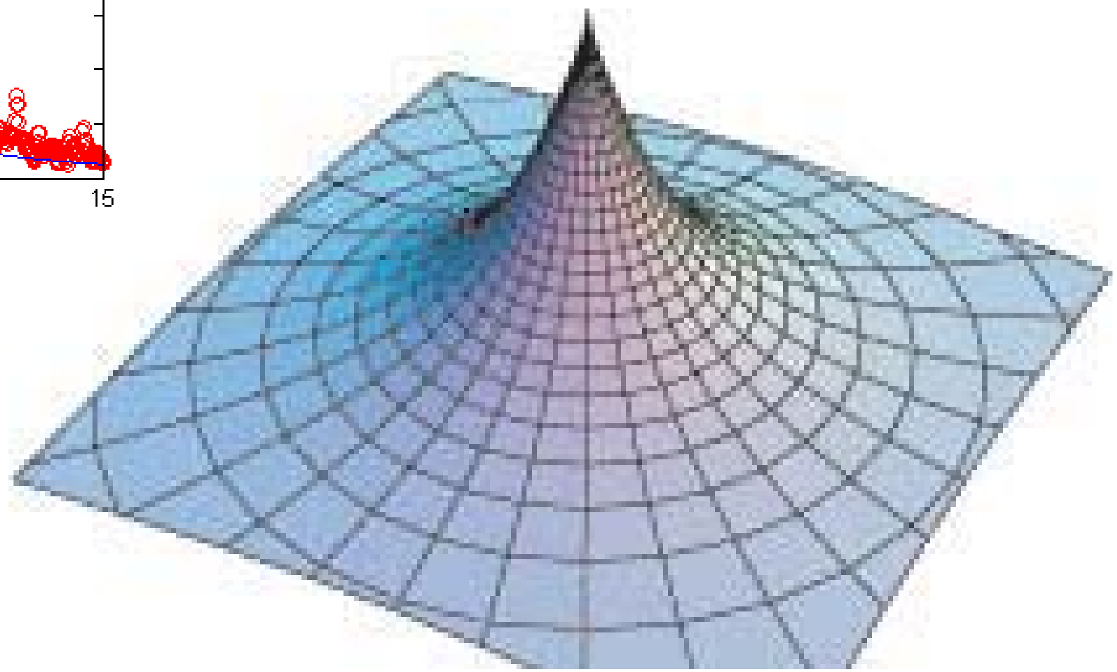

Coherent back-scattering

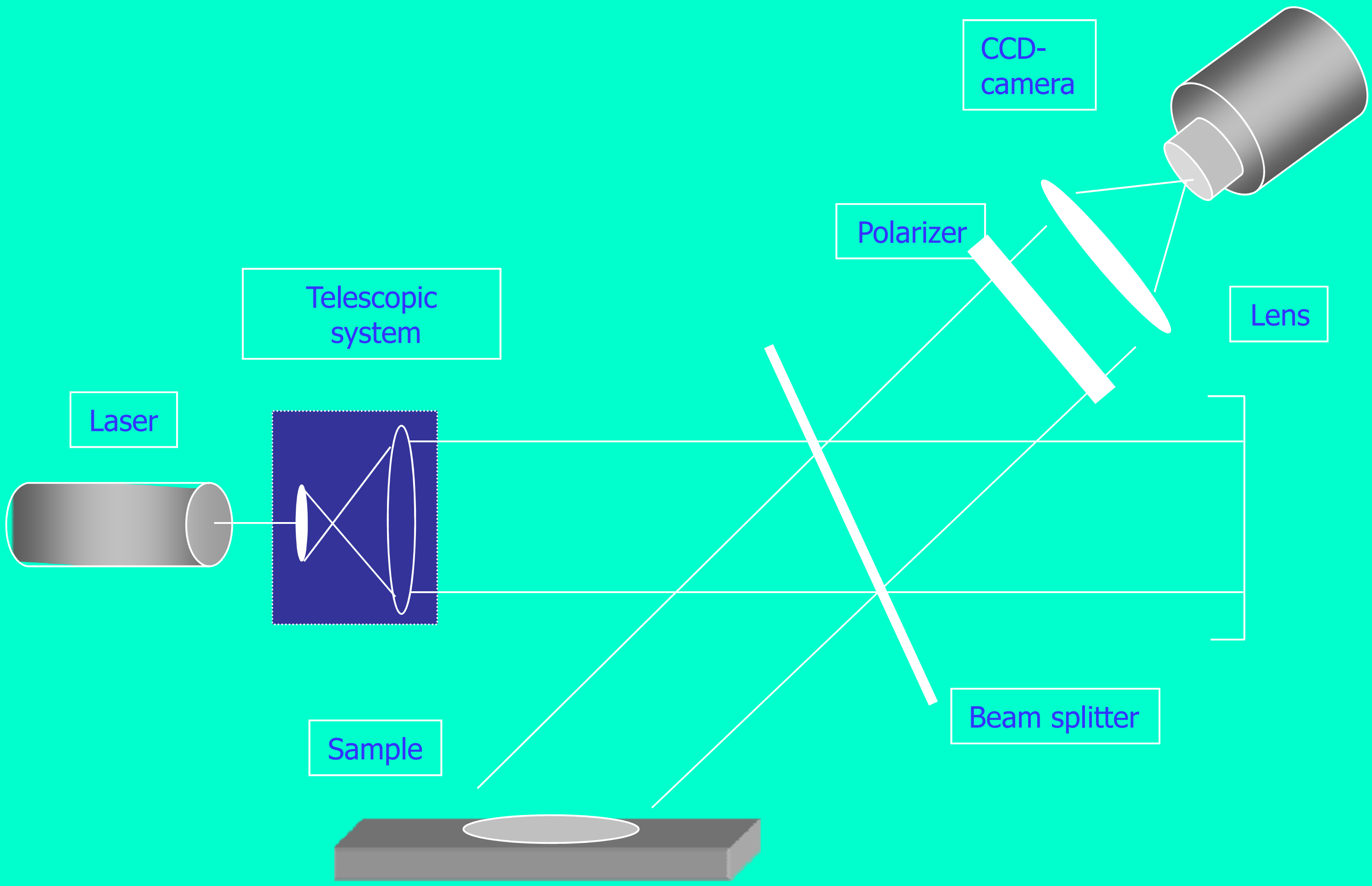

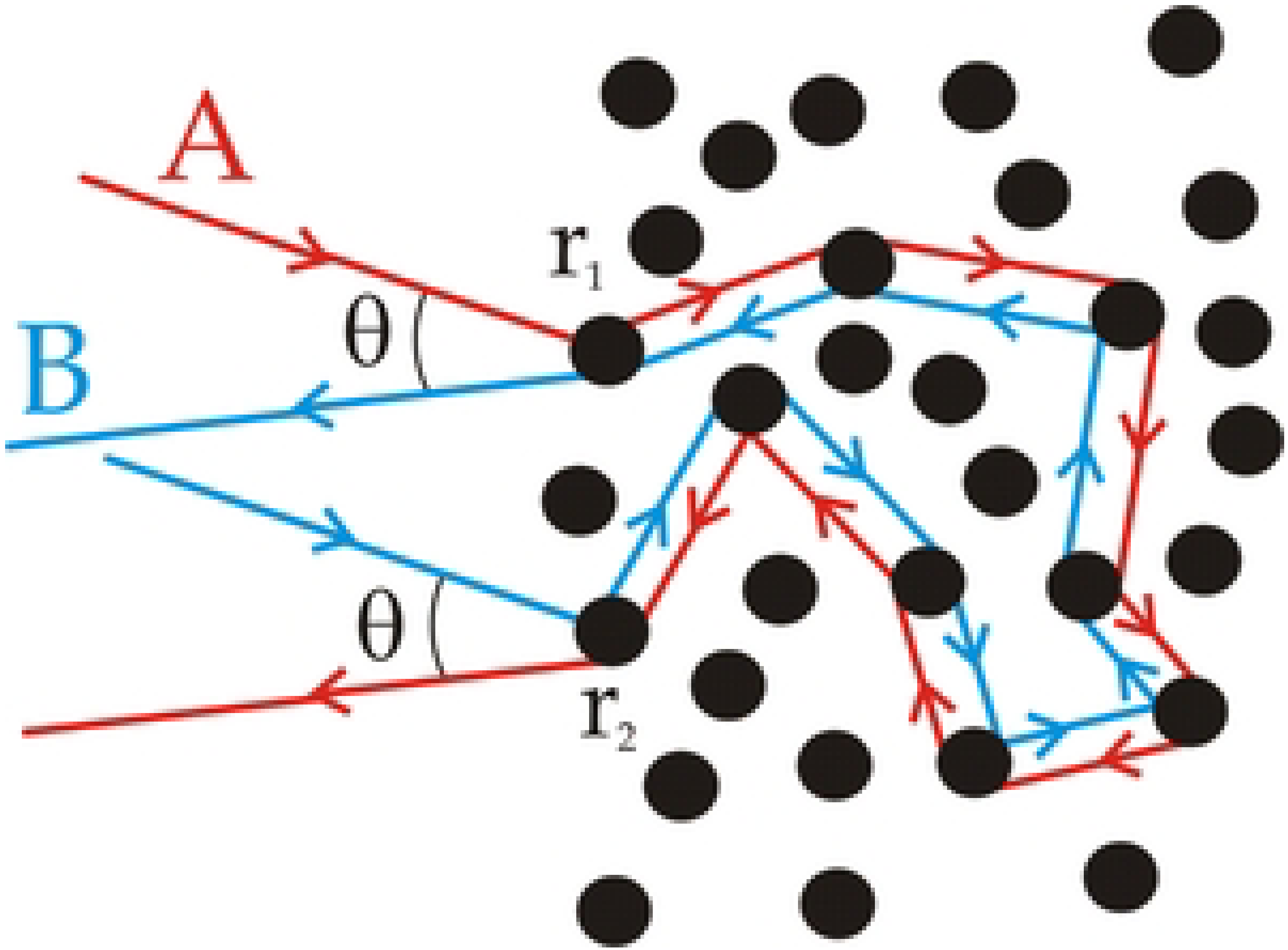
A
B
r1
r2
θ
θ

Coherent backscattering analysis

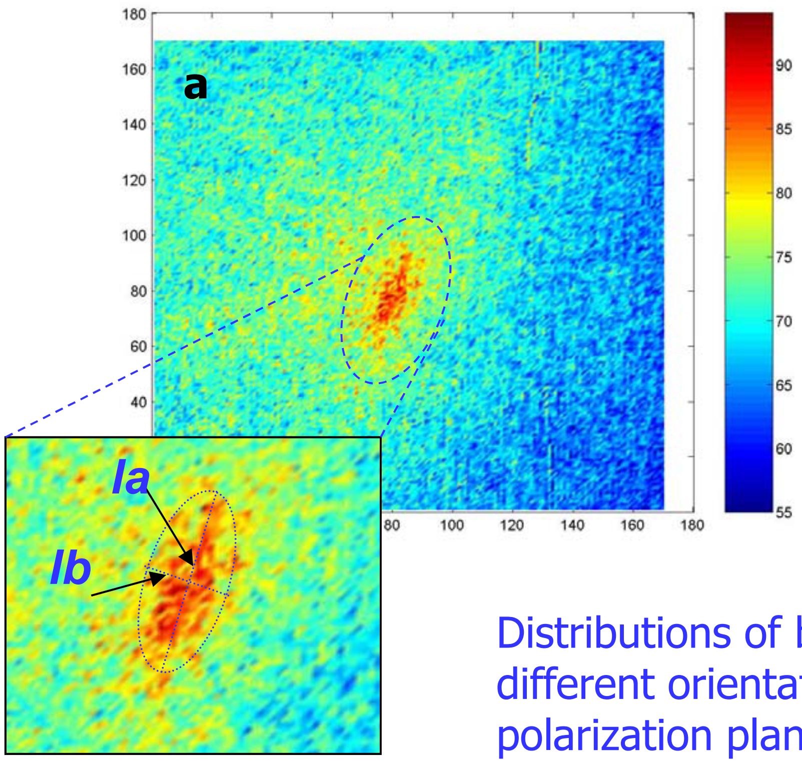

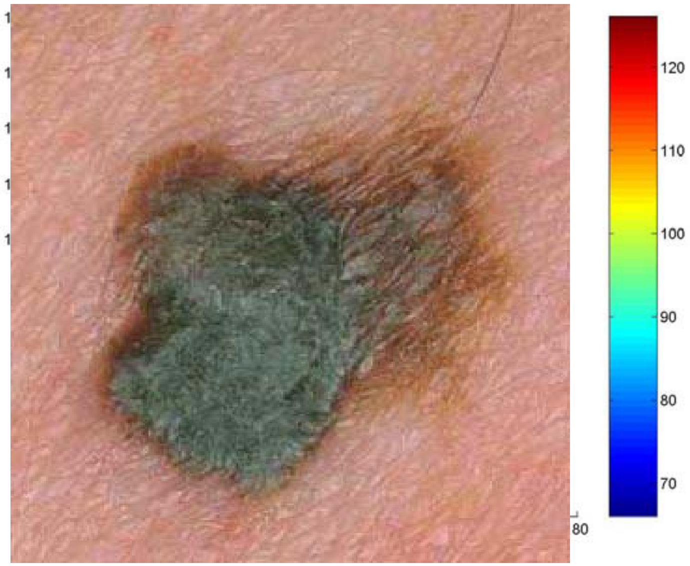

Distributions of backscattered intensity in the image plane for different orientations of the studied sample with respect to polarization plane of laser beam

$$\mu'_{s,x} / \mu'_{s,y} = (l_a / l_b)^{-2} = 0,37$$

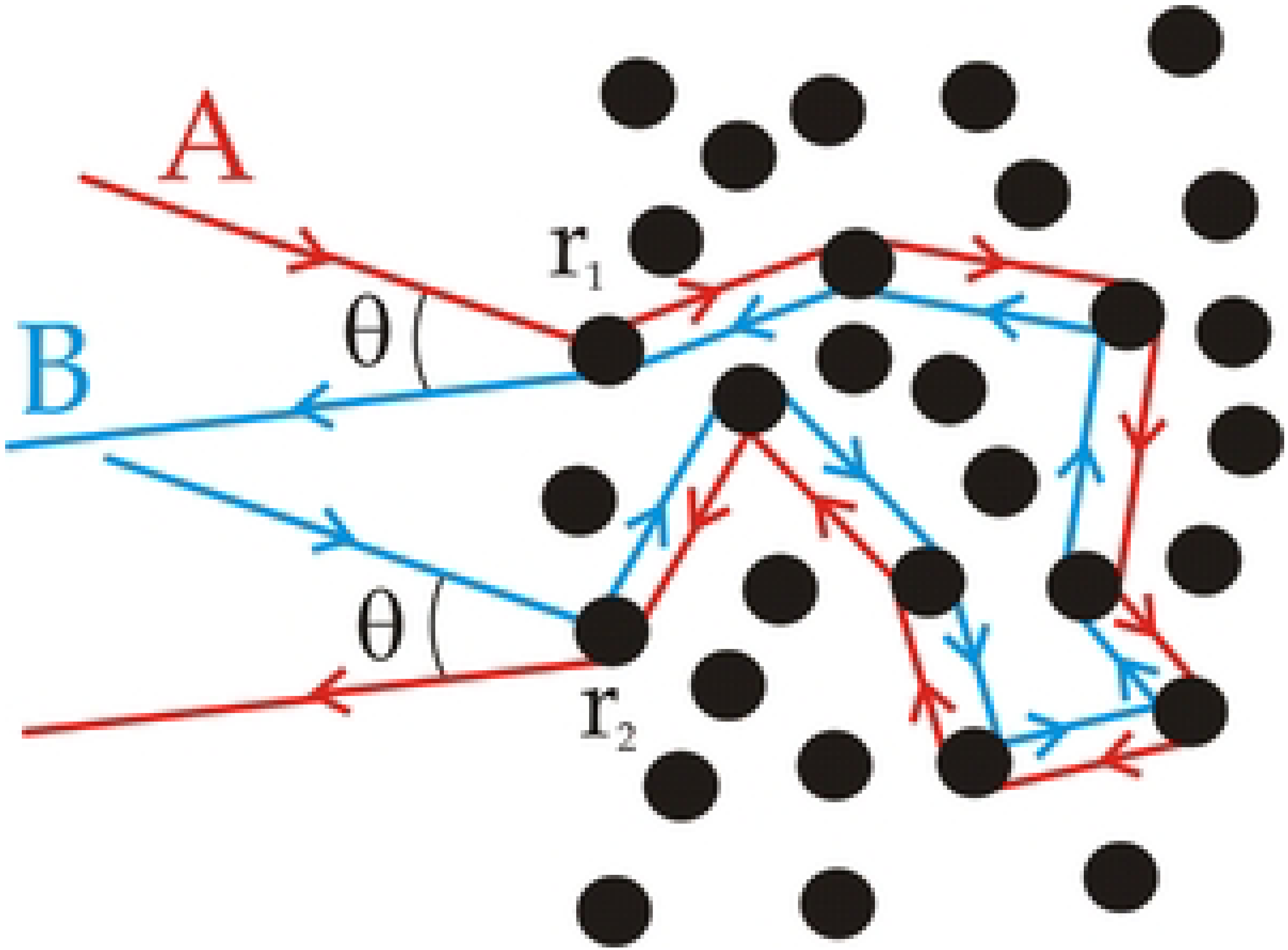
A
B
θ
θ
r_1
r_2

Diffusing Wave Spectroscopy (DWS)

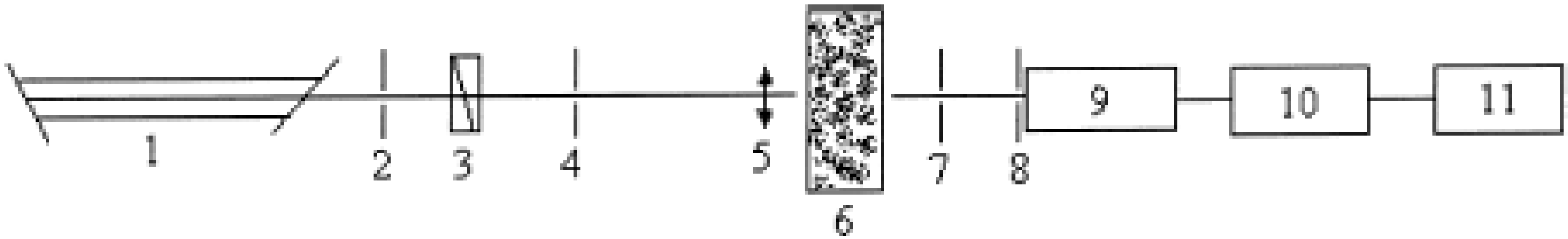

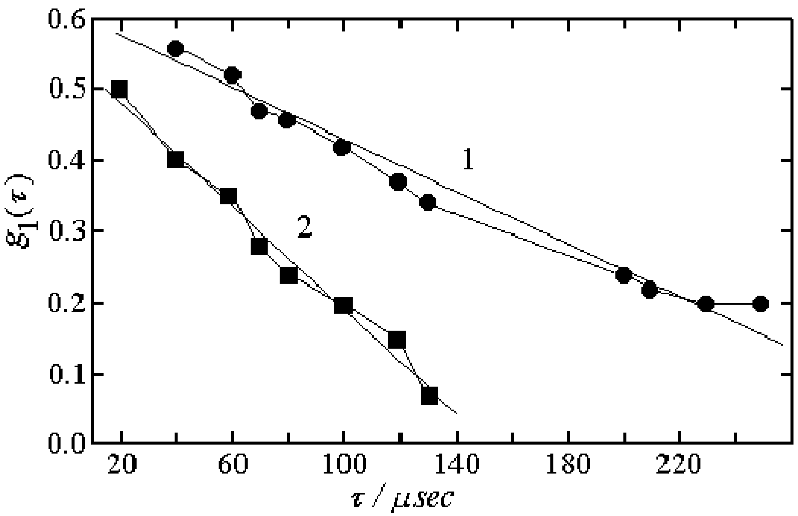

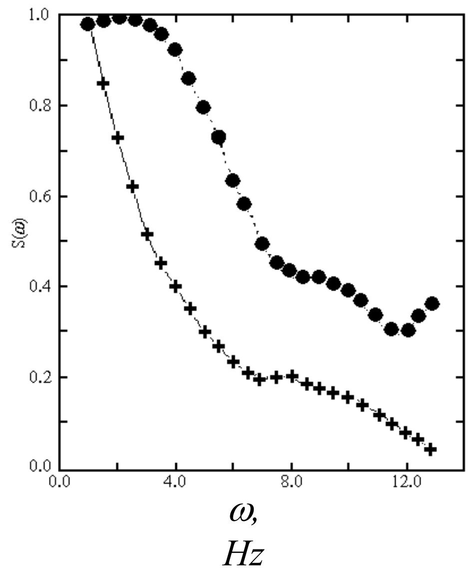

DWS principles

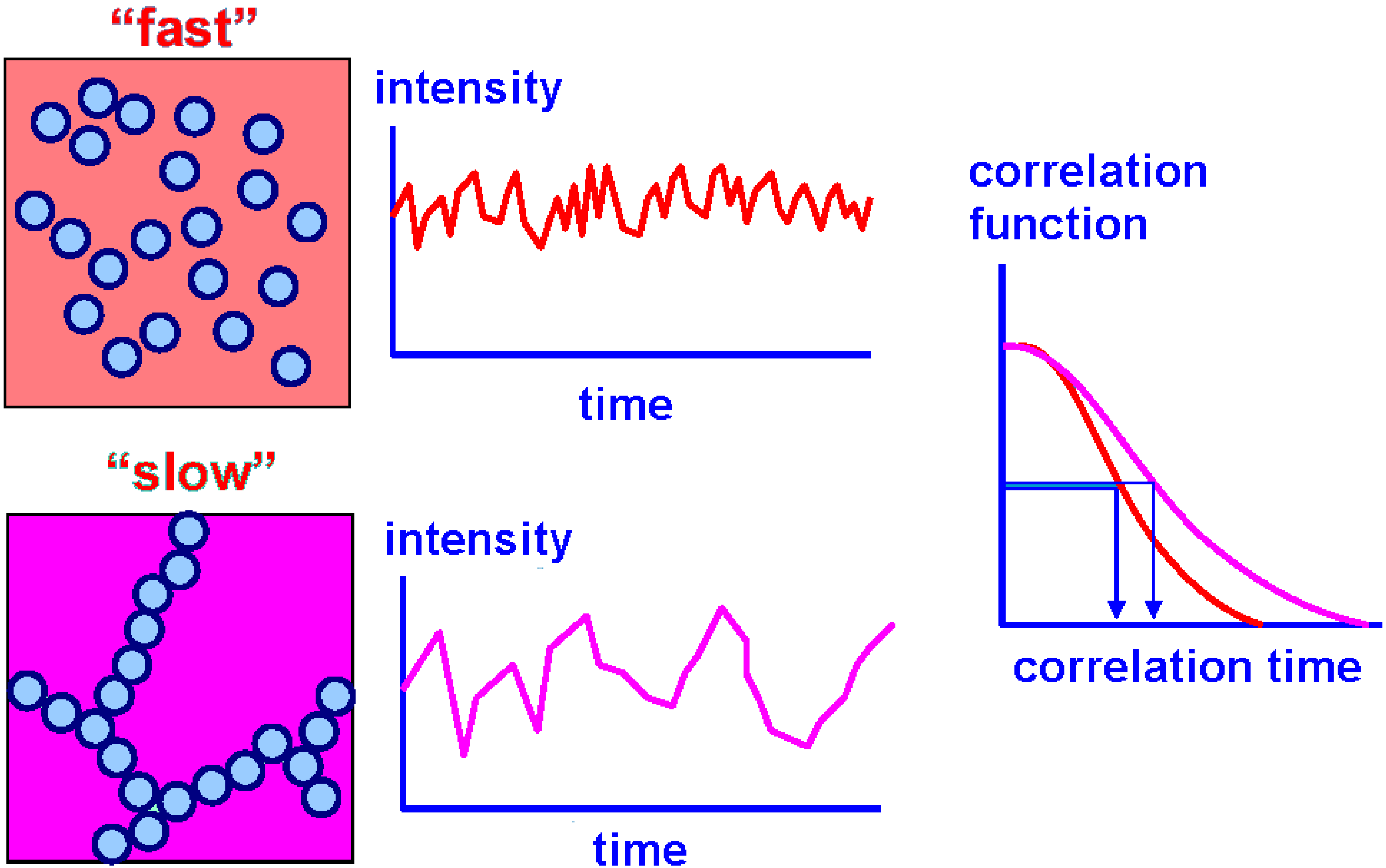

Gel dynamics

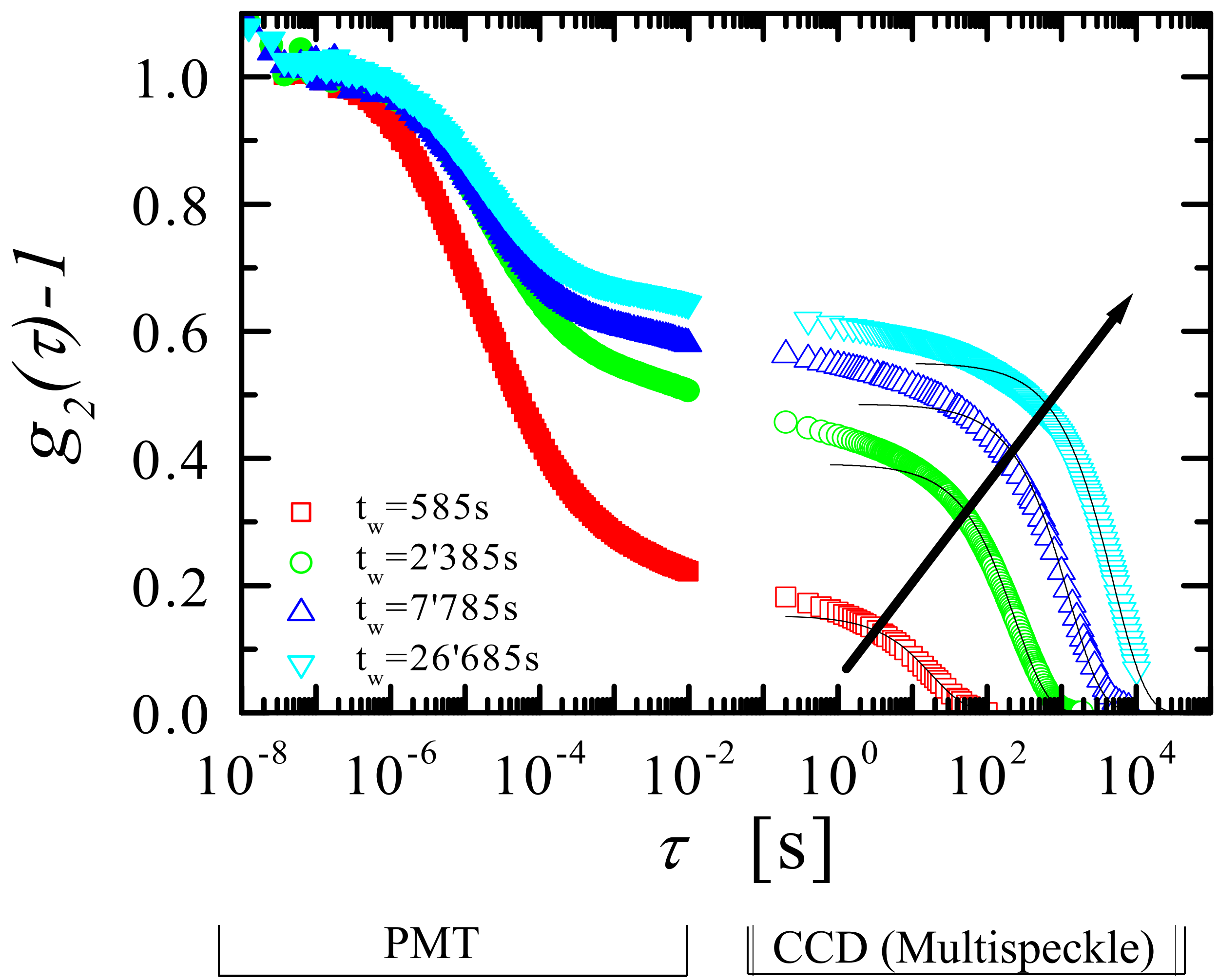

DWS experimental approach

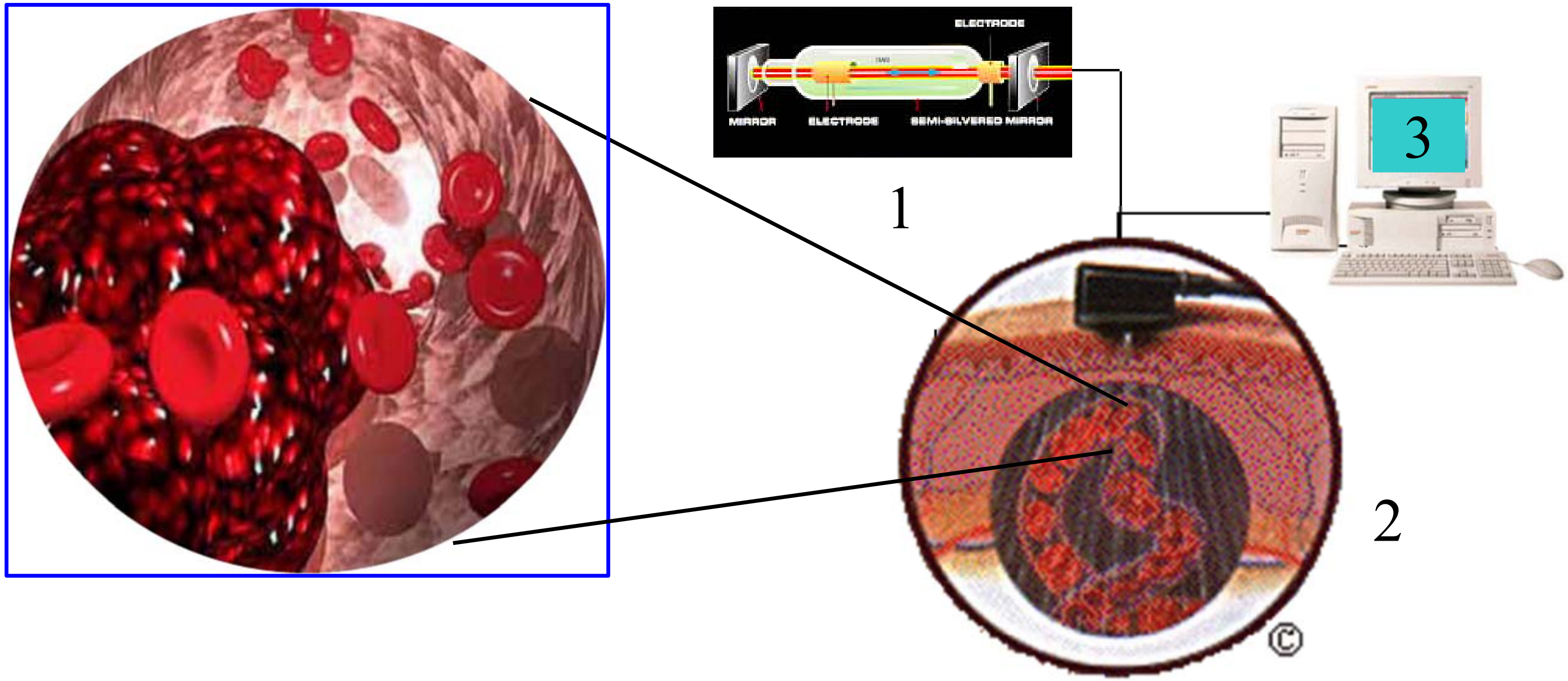

1 - laser; 2 - skin; 3 - APD, autocorrelator & PC

Why DWS?

- **Doppler ultrasound** – long acoustic wavelength required for deep tissue penetration limits spatial resolution to 200 μm
- **Capillaroscopy** requires the tissues to be thin enough (less than 400 μm) to be transilluminated
- **Confocal microscopy** can only be collected at a fraction of the normal video rate; law scattering
- **Conventional and magneto resonance angiography** provides the information mainly about large blood vessels (coronary artery, etc.)
- **Laser Doppler Flowmetry (LDF)** – strong scattering in tissue limits spatially resolved flow measurements; provide only an average characteristic of the skin blood flow (perfusion); an understanding of which vascular bed is primarily responsible for the detected signal is required
- **ODT** and **CDOCT** are highly sensitive to movement of measured object; an inability to quantify flow at resolution 50 μm or less, and/or in small vessels, where the blood flow is less than ~ 100 $\mu m/sec$.

Experimental approach

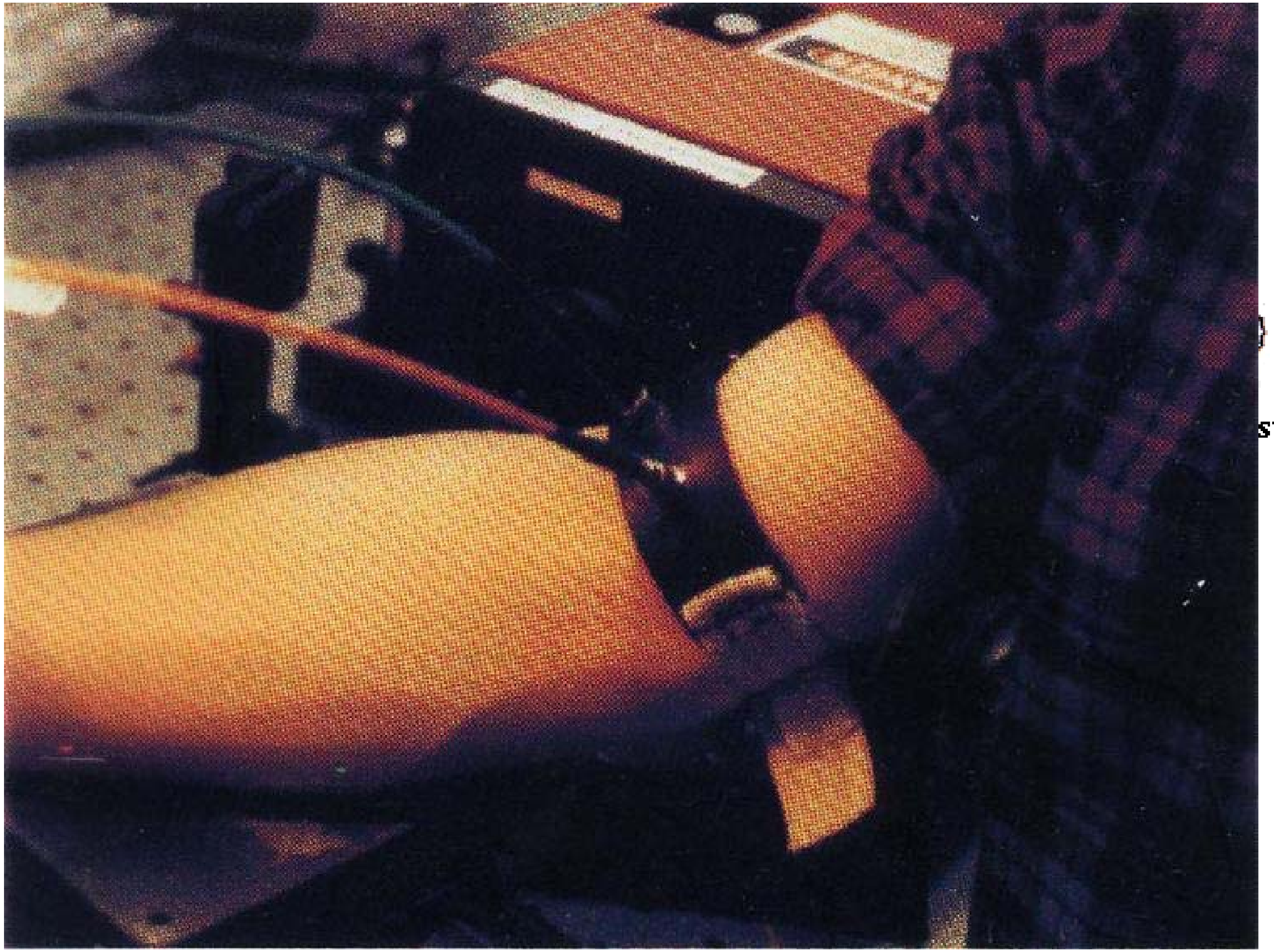

sure

Meglinski, Boas, Yodh, Chance

Experimental Results

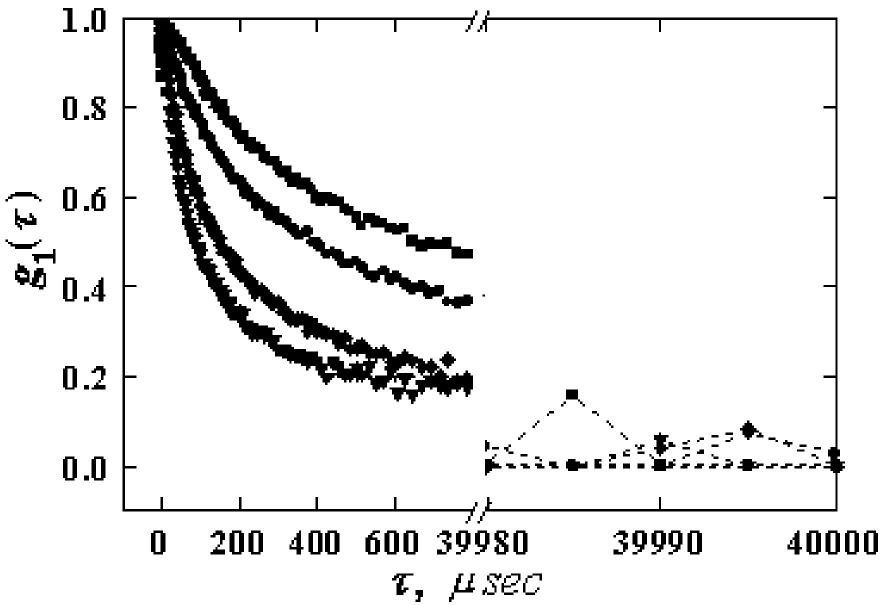

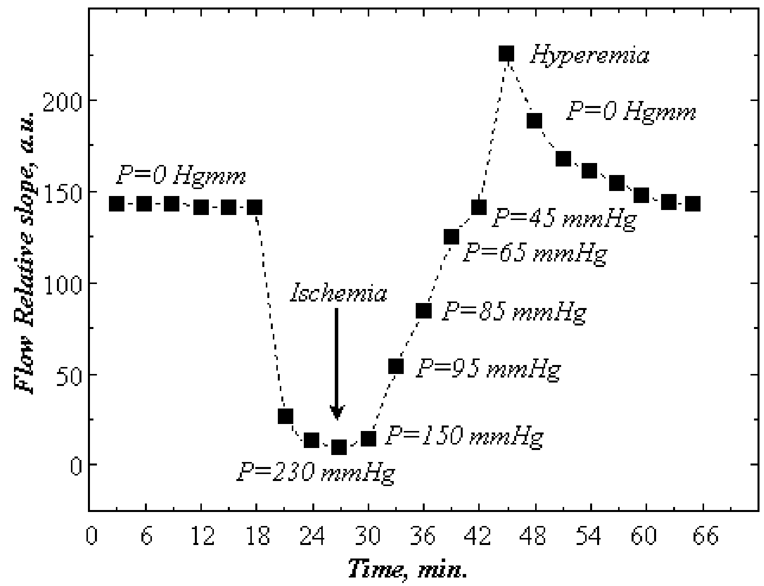

$$g_1(\tau) = \int_0^\infty P(s) \exp\left(-\frac{1}{3} k_0^2 < \Delta r^2(\tau) > \frac{s}{l^*} \right) ds$$

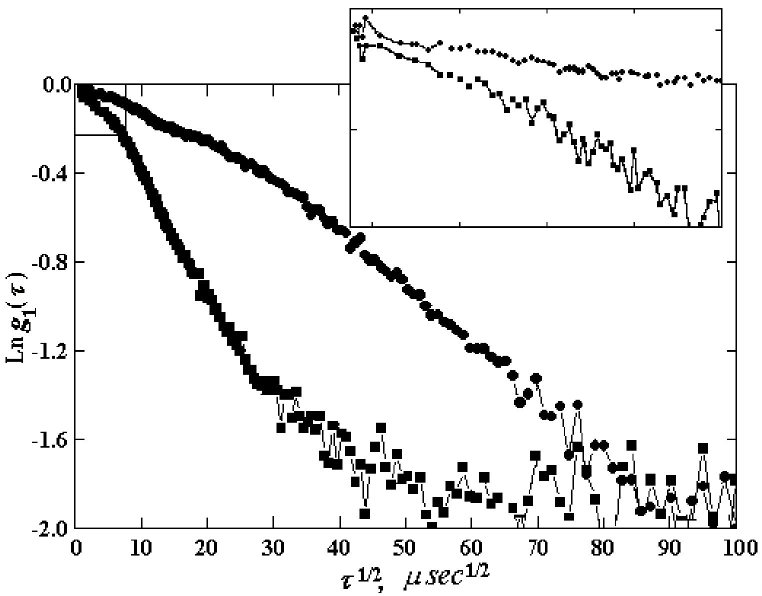
0.0
-0.4
-0.8
-1.2
-1.6
-2.0
Ln $g_1(\tau)$
0 10 20 30 40 50 60 70 80 90 100
$\tau^{1/2}$, $\mu sec^{1/2}$

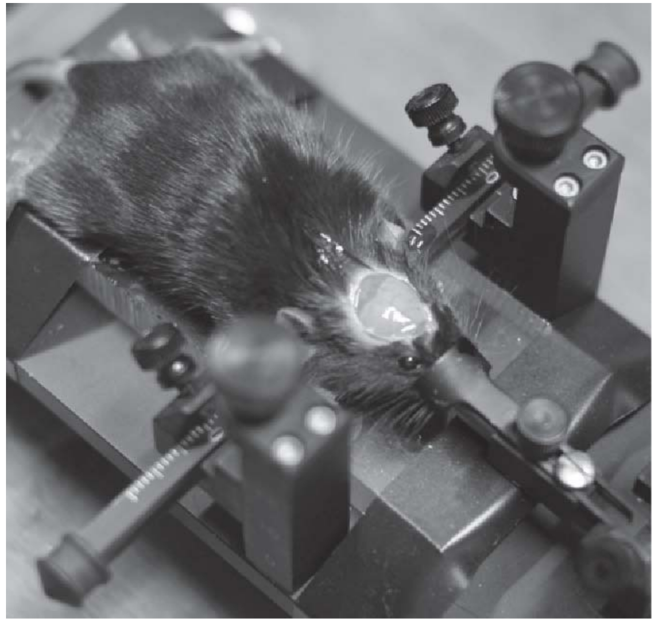

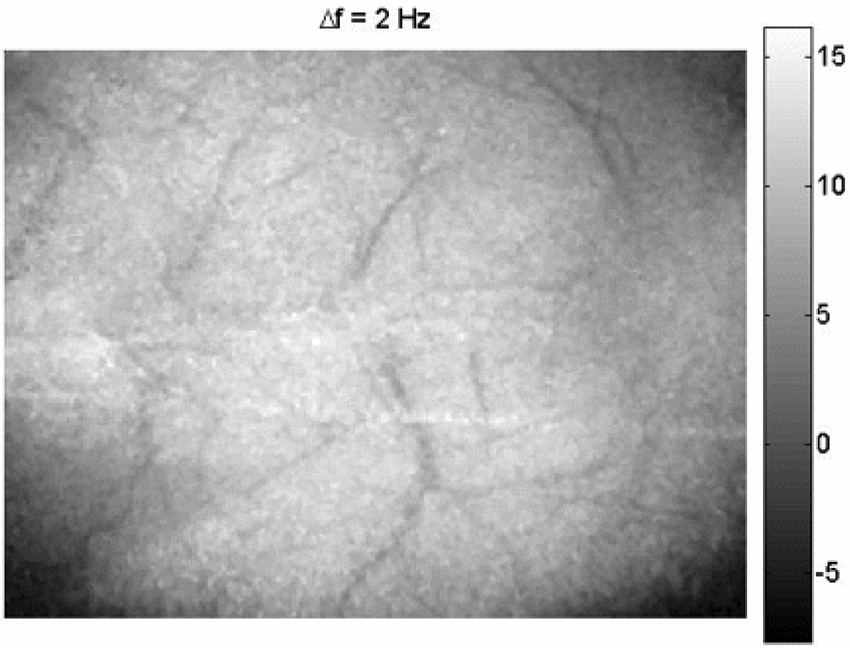
Δf = 2 Hz
15
10
5
0
-5

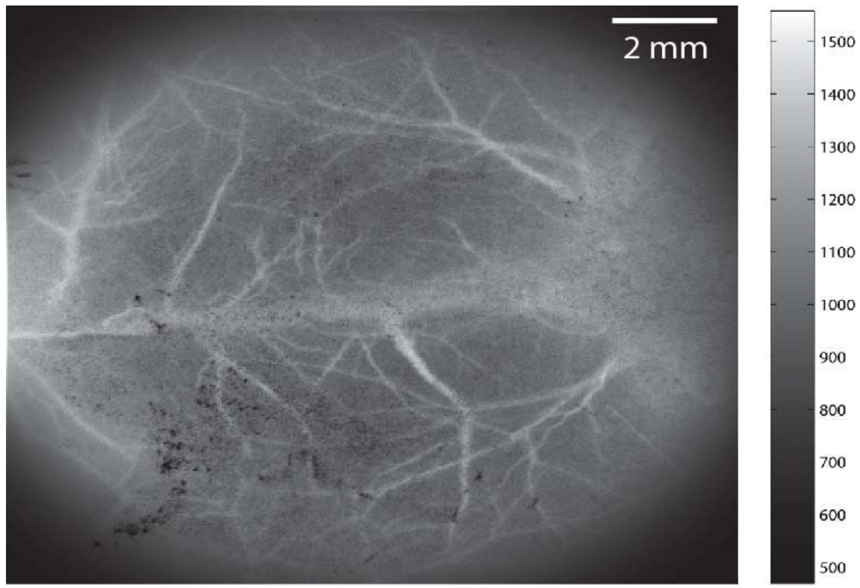
2 mm
1500
1400
1300
1200
1100
1000
900
800
700
600
500

Experimental Results

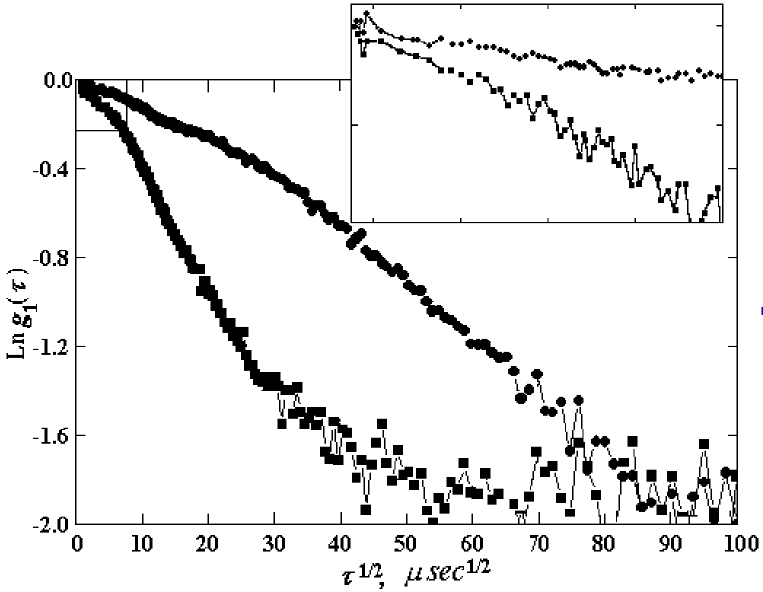

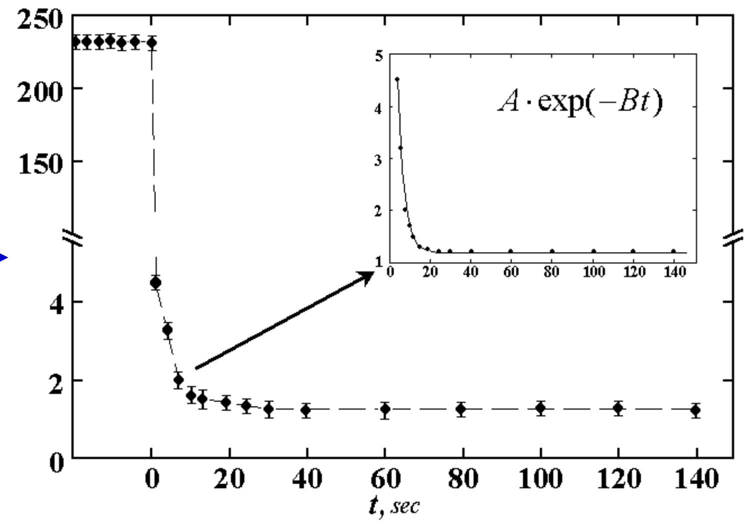

Meglinski, Tuchin (2001)

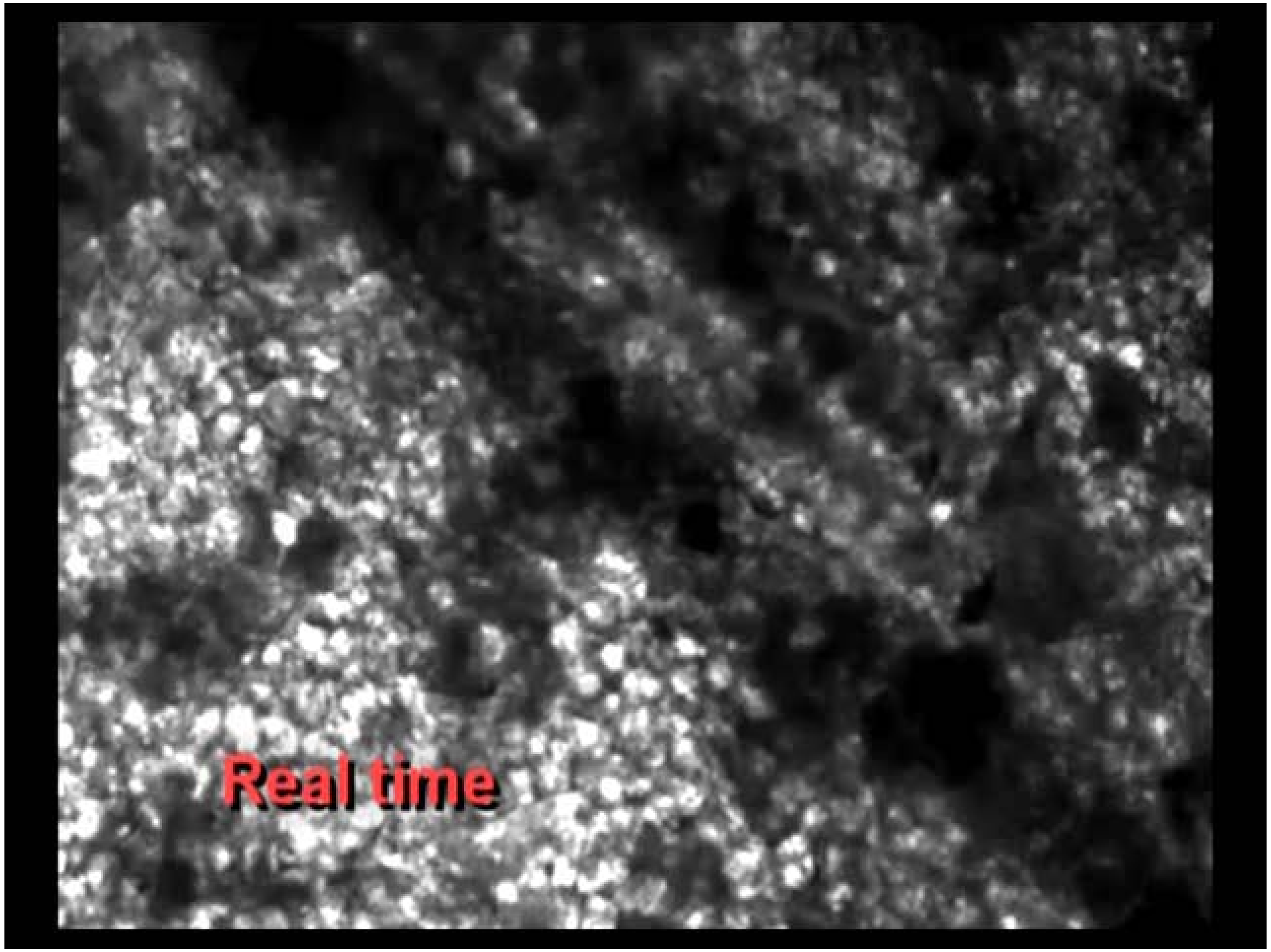
Real time

Laser Doppler or LASCA skin blood imaging

before occlusion | during occlusion | after occlusion

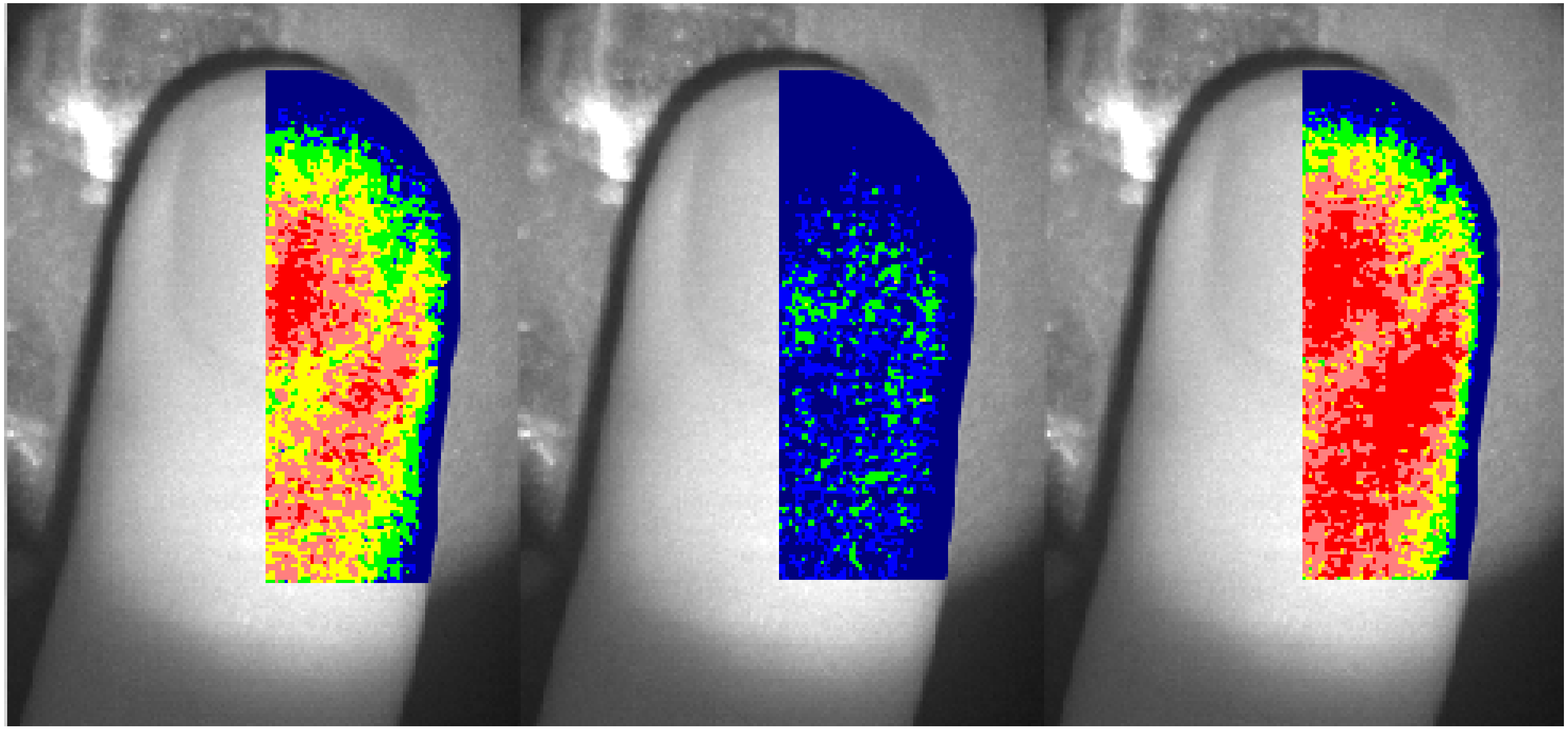

Laser Doppler Perfusion

LOW HIGH

Results of simulation

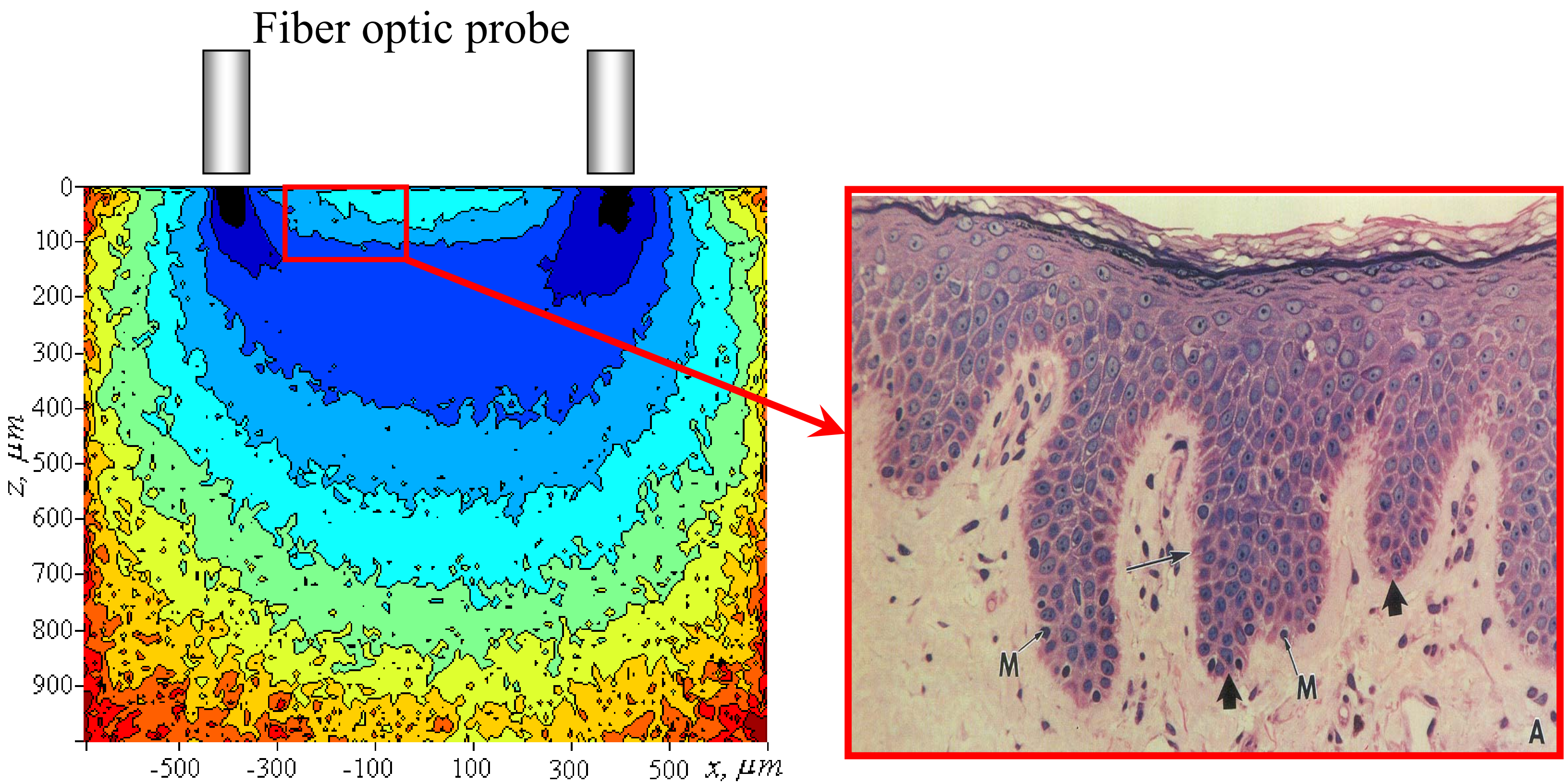

Siegert´s relation

Einsteins theory describes the *electric field* correlation function, $g_1(t)$.

DWS/PCS experiments probes the *intensity* correlation function $g_2(t)$.

$I(t)=E(t)\,E^*(t)$

$+$

Gaussian approximation

$$\boxed{g_2(t) = 1 + \sigma \left| g_1(t) \right|^2}$$

Polarisation vector MC model

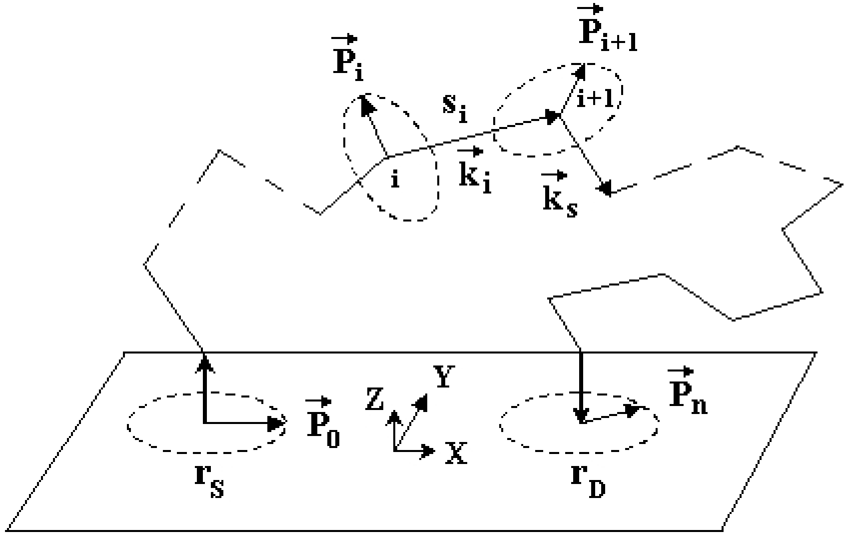

Polarisation vector

$$\mathbf{P}^{out} = \prod_j \left(\hat{I} - \frac{(\mathbf{R}_{j+1} - \mathbf{R}_j) \otimes (\mathbf{R}_{j+1} - \mathbf{R}_j)}{|\mathbf{R}_{j+1} - \mathbf{R}_j|^2} \right) \mathbf{P}^{(in)}$$

Co- and cross-polarised components

$$I_{x\,\alpha} = \sum_{i=1}^{N_{ph}} W_i P_{i\,\alpha}^{out\,2} R_R^{n_i}$$

Rayleigh factor

$$R_R = 2(1 + \overline{\cos^2\theta})^{-1}$$

Polarization Algorithm

$$I_{pol} = I_{XX} = \sum_{i=1}^{N_{ph}} W_{di} \boxed{P_{i\,x}^{2} \Gamma_{R}^{n_i}}$$

$$I_{depol} = I_{YX} = \sum_{i=1}^{N_{ph}} W_{di} \boxed{P_{i\,y}^{2} \Gamma_{R}^{n_i}}$$

Kuzmin, Meglinski, Churmakov (2005) ***Optics & Spectroscopy***

Polarisation

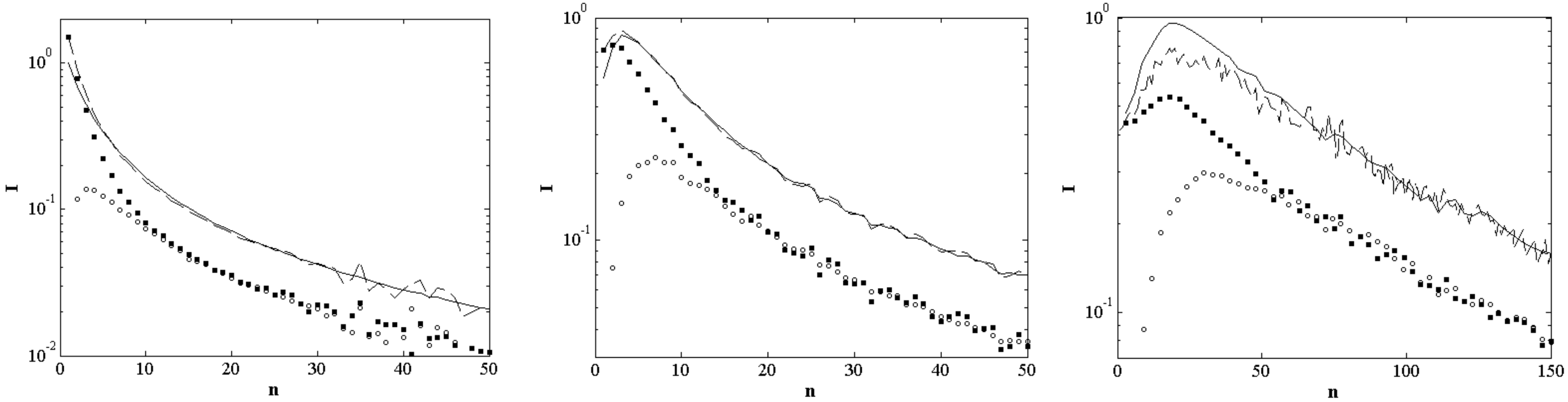

Co-polarised (■) and Cross-polarised (○) components as a function of the number of scatterings *n* for different anisotropy factors: a) g = 0, b) g = 0.5, c) g = 0.9. Semi-infinite medium. Infinite detector with NA = 0.

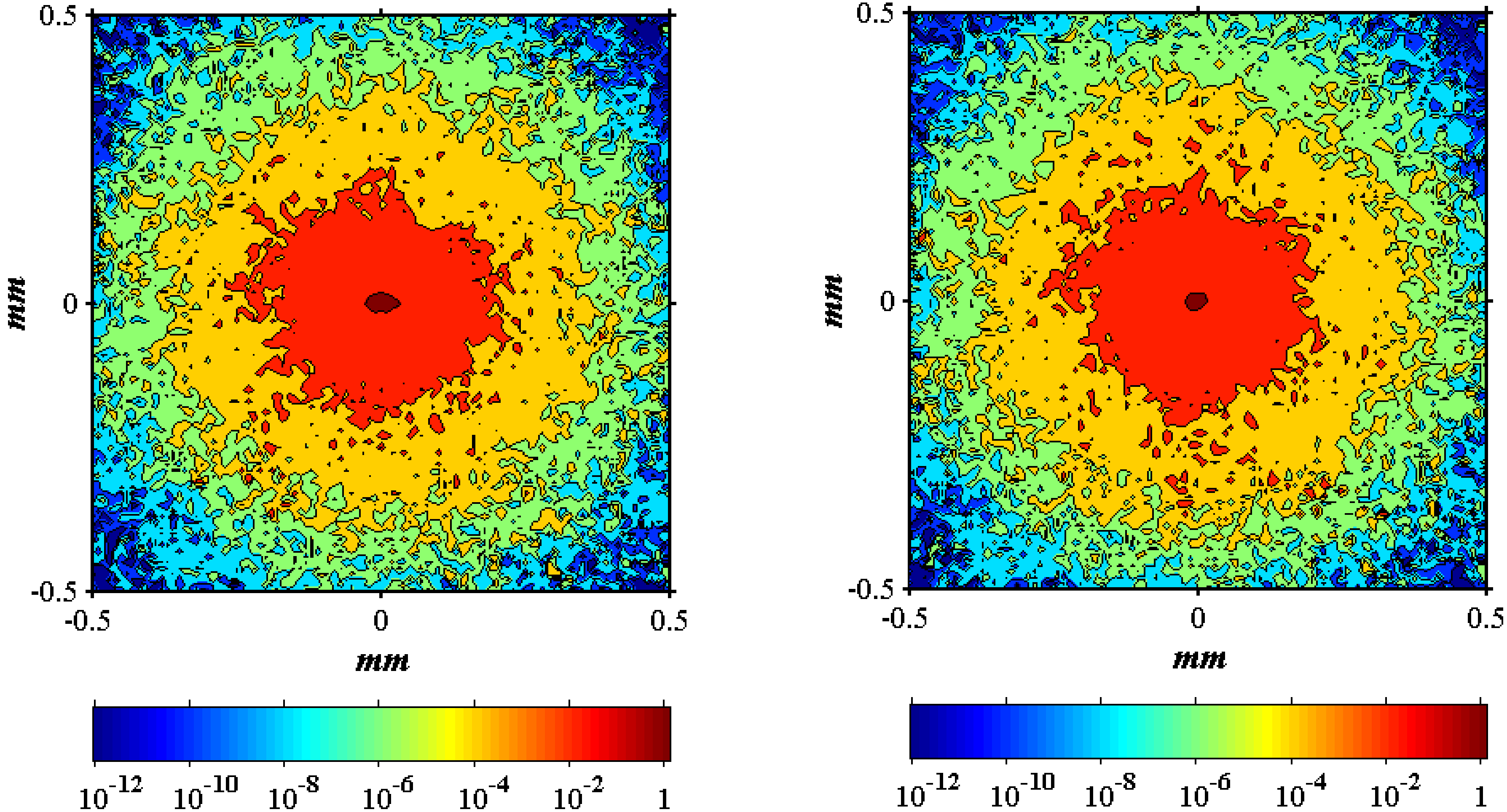

$$I_{pol} = I_{XX} = \sum_{i=1}^{N_{ph}} W_{di} P_{i\,x}^{2} \Gamma_{R}^{n_i}$$

$$I_{depol} = I_{YX} = \sum_{i=1}^{N_{ph}} W_{di} P_{i\,y}^{2} \Gamma_{R}^{n_i}$$

Results of Simulation

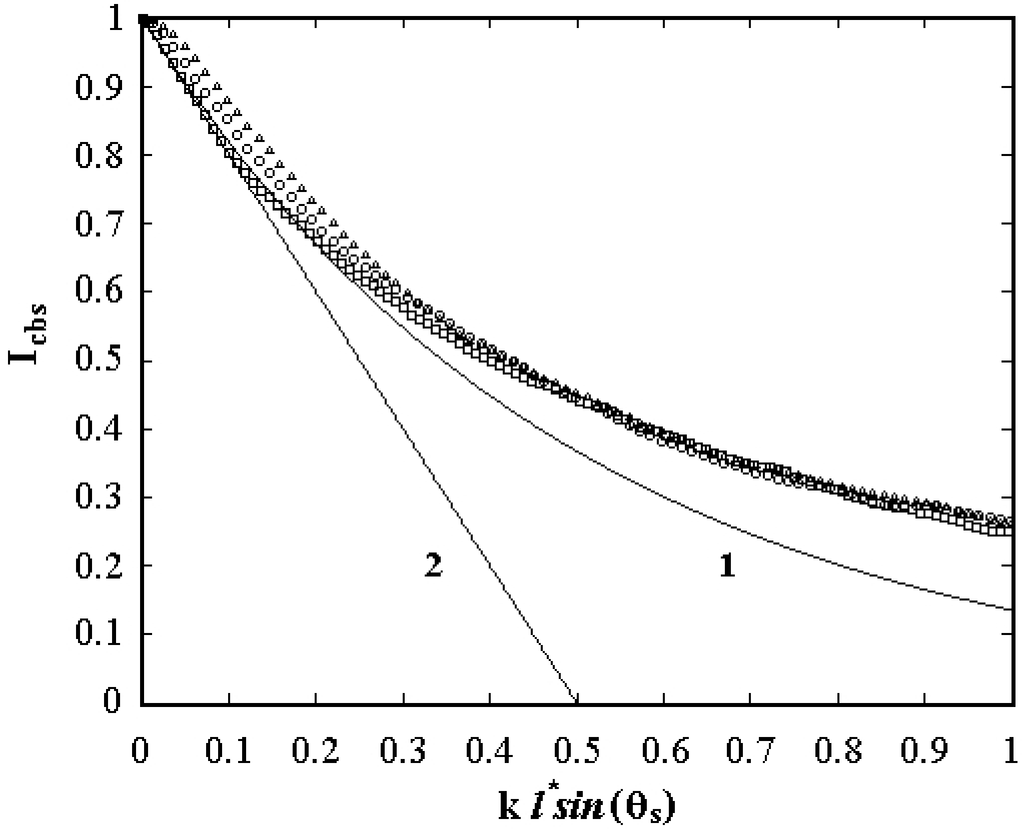

$$1 - \quad I^{CBS} = \exp(-\gamma k l^{*} \sin\theta_s)$$

$$2 - \quad I^{CBS} = 1 - \gamma k l^{*} \sin\theta_s$$

Figure 5. The peak of CBS ($I_{\rm CBS}$) as a function of $kl^{*} \sin\theta_{\rm s}$: $\square$, $\langle\cos\theta\rangle = 0$; $\circ$, $\langle\cos\theta\rangle = 0.5$; $\blacktriangle$, $\langle\cos\theta\rangle = 0.9$. Solid lines represent (1) equation (5.2) and (2) equation (5.3).

Meglinski, *et al.*, *Proc. Roy. Soc. A* (2005)

Validation

	Milne-type solution	**MC results**
Isotropic	4.227.. (van Rossum, Nieuwenhuizen 1999)	4.22 ± 0.05
Anisotropic	4.88, $g \to 1$ (Amic, et al. 1996)	4.6 ± 0.2, g = 0.9
Rayleigh, Polarized component	3.05 (Amic, et al, 1997; Kuzmin, Aksenova, 2003)	3.05 ± 0.05
Rayleigh, De-polarized component	1.59 (Amic, et al, 1997; Kuzmin, Aksenova, 2003)	1.55 ± 0.05

Polarisation

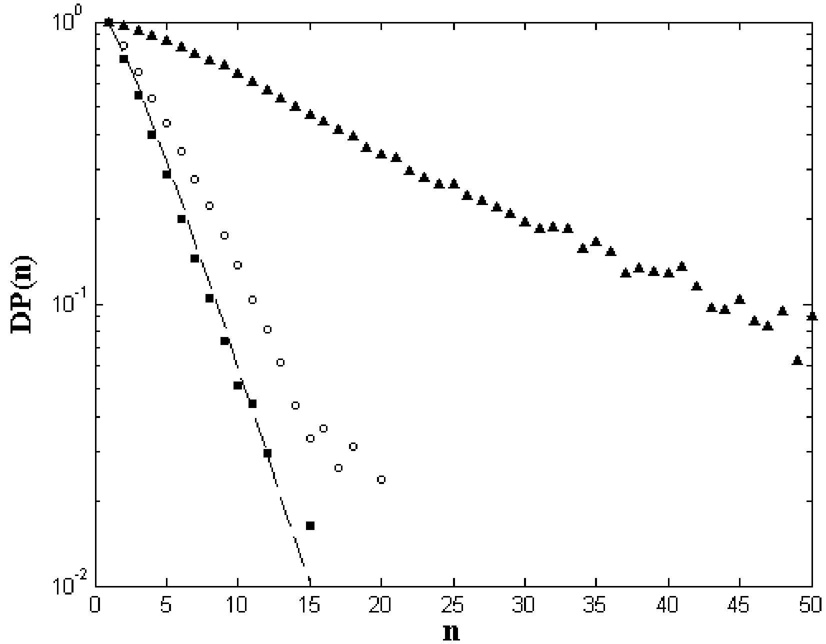

Depolarisation factor *DP*(*n*) for different anisotropy factors: (■) g = 0, (○) g = 0.5, (▲) g = 0.9. Dashed line is the theoretical predictions (Akkermans, *et al.*, *J. Physics France*, 1988).

Validation

Source	Detector	Milne solution	Diffusion approximation	MC
Plain wave	Plain wave	2	$2\dfrac{(1+z')^2}{1+2z'}$	1.98
Plain wave	Point detector	1.53	$1+z'$	1.53
Point source	Point detector	0.95		1.1

$z' = z^*/l_s\ ,\ z^* \sim 0.71 l_s$

Kuzmin, Churmakov, Meglinski (2005)

Polarization Algorithm

$$I_{pol} = I_{XX} = \sum_{i=1}^{N_{ph}} W_{di} \boxed{P_{i\,x}^{2} \Gamma_{R}^{n_i}}$$

$$I_{depol} = I_{YX} = \sum_{i=1}^{N_{ph}} W_{di} \boxed{P_{i\,y}^{2} \Gamma_{R}^{n_i}}$$

$$g_{pol}^{(1)}(t) = g_{XX}^{(1)}(t) = \sum_{i=1}^{N_{ph}} W_{di} \boxed{P_{i\,x}^{2} \Gamma_{R}^{n_i}} \exp(-2\frac{t}{\tau} n_i (1 - \frac{1}{n_i} \sum_{j=1}^{n_i} \cos\theta_j))$$

$$g_{depol}^{(1)}(t) = g_{YX}^{(1)}(t) = \sum_{i=1}^{N_{ph}} W_{di} \boxed{P_{i\,y}^{2} \Gamma_{R}^{n_i}} \exp(-2\frac{t}{\tau} n_i (1 - \frac{1}{n_i} \sum_{j=1}^{n_i} \cos\theta_j))$$

Kuzmin, Meglinski, Churmakov (2005) ***Optics & Spectroscopy***

Results of Simulation

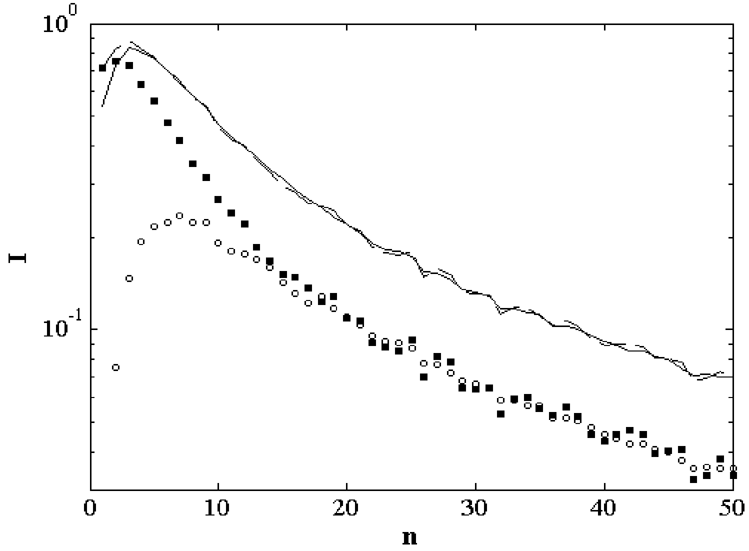

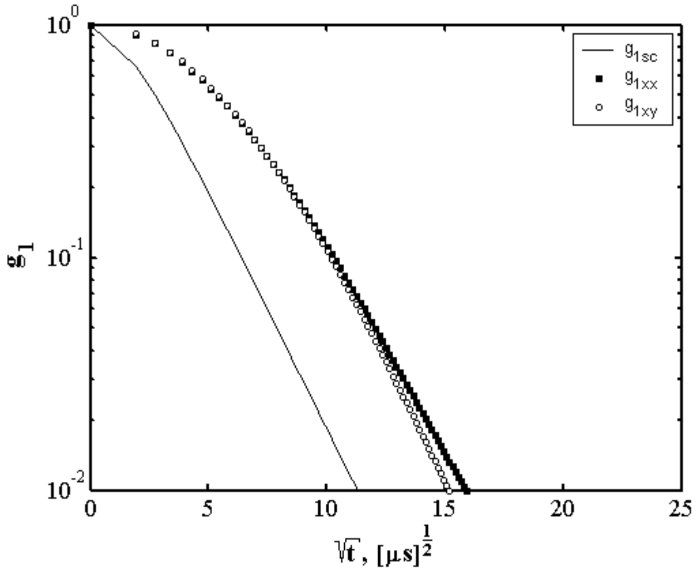

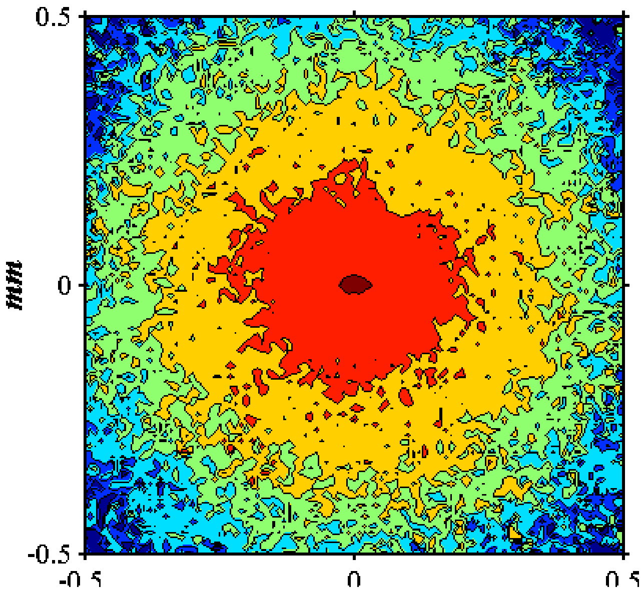

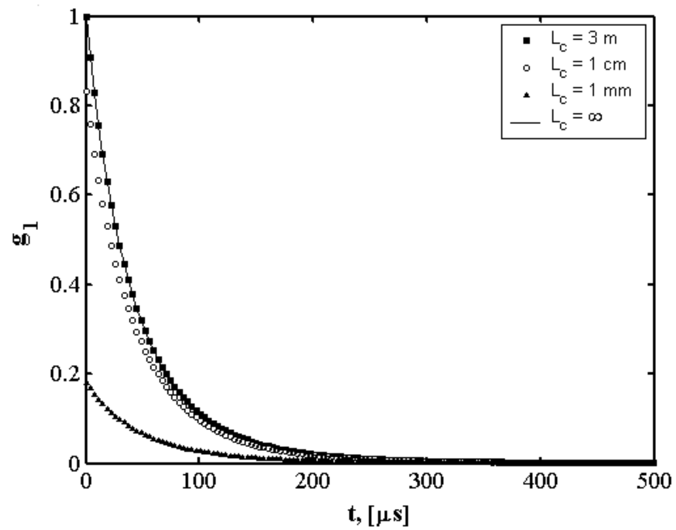

Results

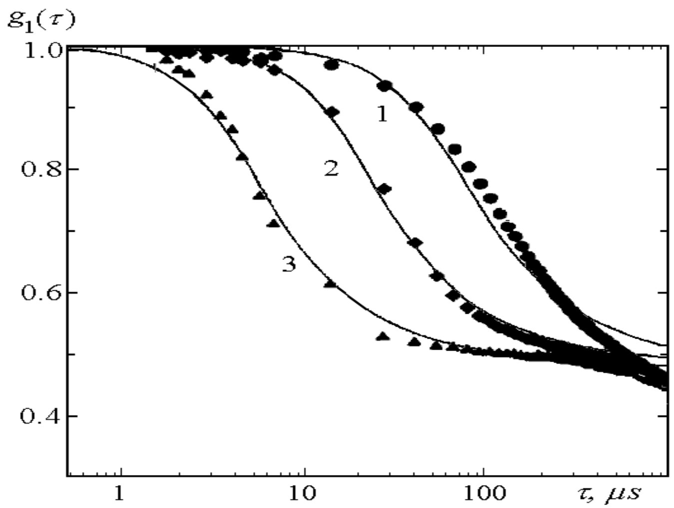

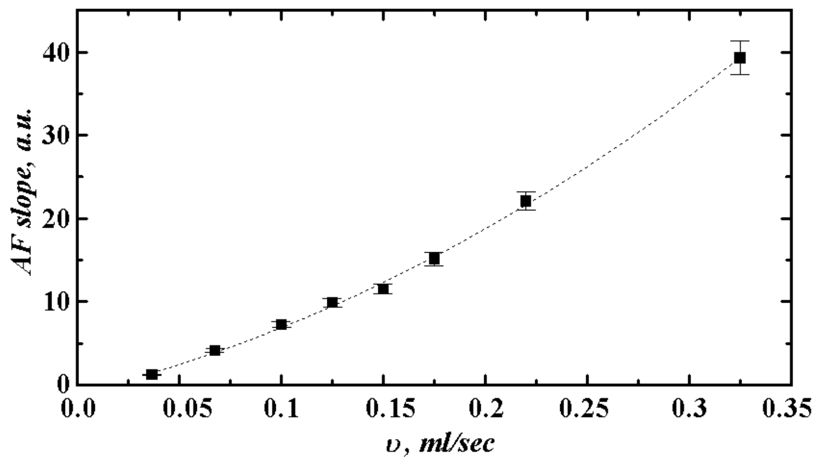

Meglinski, Tuchin (2004)

Summary

Based on the combination of the MC technique and the solution to the Bethe–Salpeter equation, it has been shown that it is possible to employ a unified approach describing the coherence effects in randomly inhomogeneous disperse multiple scattering media. The results of simulation demonstrate a good agreement with the DWS theory. They are also in good agreement with the experimental results (Pine *et al*. 1988; MacKintosh & John 1989) and the results of an alternative simulation (Lenke *et al*. 2002). Potential applications of this modelling technique are various studies of suspensions, liquid crystals, biological tissues, etc.

Challenges and the needs of Bio-Medicine

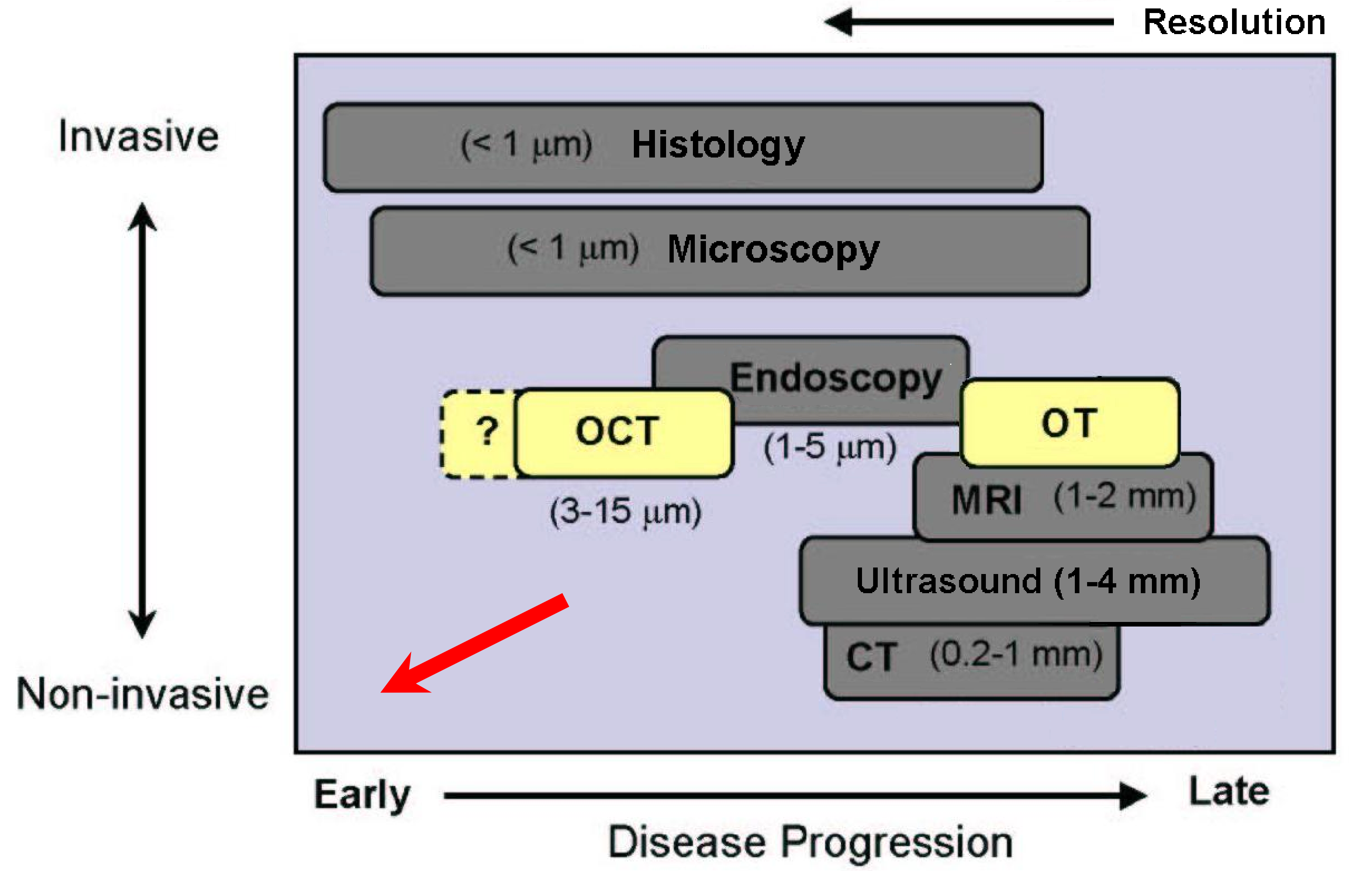

OCT and PS OCT

Polarisation vector MC model

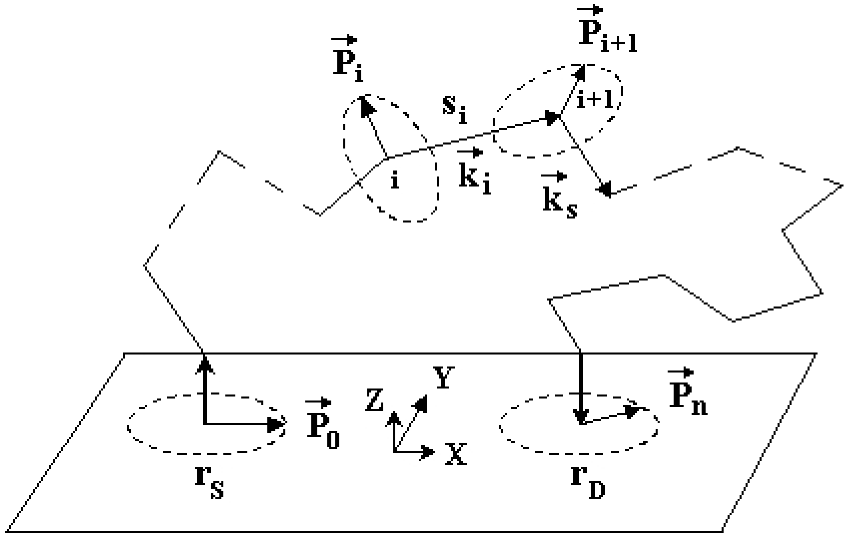

Polarisation vector

$$\mathbf{P}^{\,out} = \prod_j \left(\hat{I} - \frac{(\mathbf{R}_{j+1} - \mathbf{R}_j) \otimes (\mathbf{R}_{j+1} - \mathbf{R}_j)}{|\mathbf{R}_{j+1} - \mathbf{R}_j|^2} \right) \mathbf{P}^{(in)}$$

Co- and cross-polarised component

$$I_{x\,\alpha} = \sum_{i=1}^{N_{ph}} W_i P_{i\,\alpha}^{out\,2} R_R^{n_i}$$

Rayleigh factor

$$R_R \;=\; 2(1 + \overline{\cos^2\theta})^{-1}$$

PS-OCT MC model

$$I_{oct\ \alpha}(\tau) = \sum_{i=1}^{N_{ph}} W_i P_{i\,\alpha}^{out} \sqrt{R_R^{n_i}} \cos\left(\frac{2\pi}{\lambda}\Delta L\right) \exp\left[-4\log 2\left(\frac{\Delta L}{l_c}\right)^2\right]$$

OCT Monte Carlo

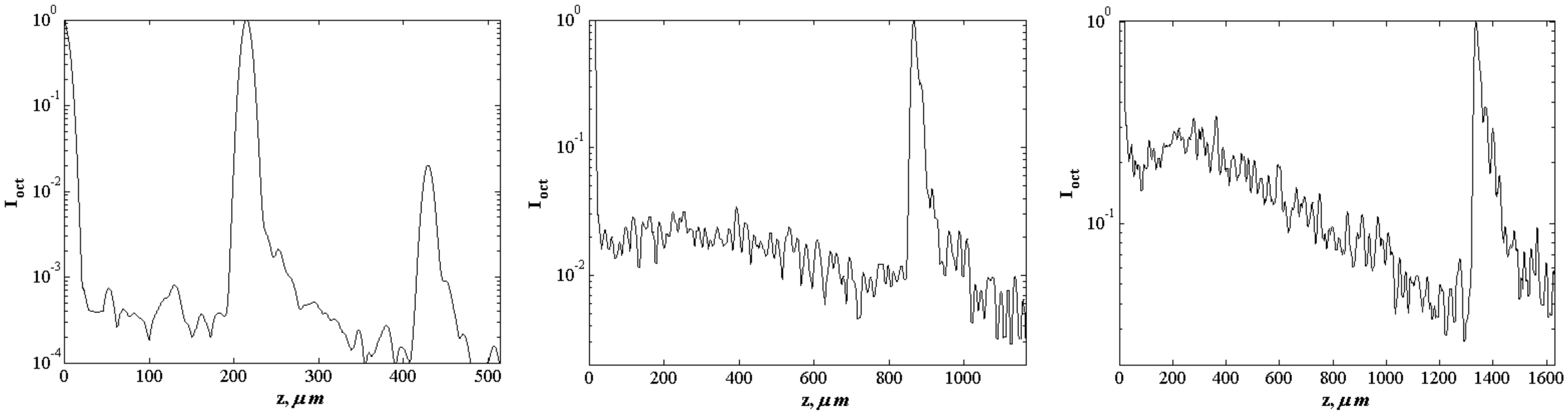

Results of PS-OCT MC model for a finite slab of different Optical Density (OD) - $2\mu_s d$: a) OD = 2, b) OD = 8, c) OD = 12.
Optical parameters: $\mu_s = 6.2\ \mu m$, g = 0.85, n = 1.33.

Results of PS OCT Images Simulation

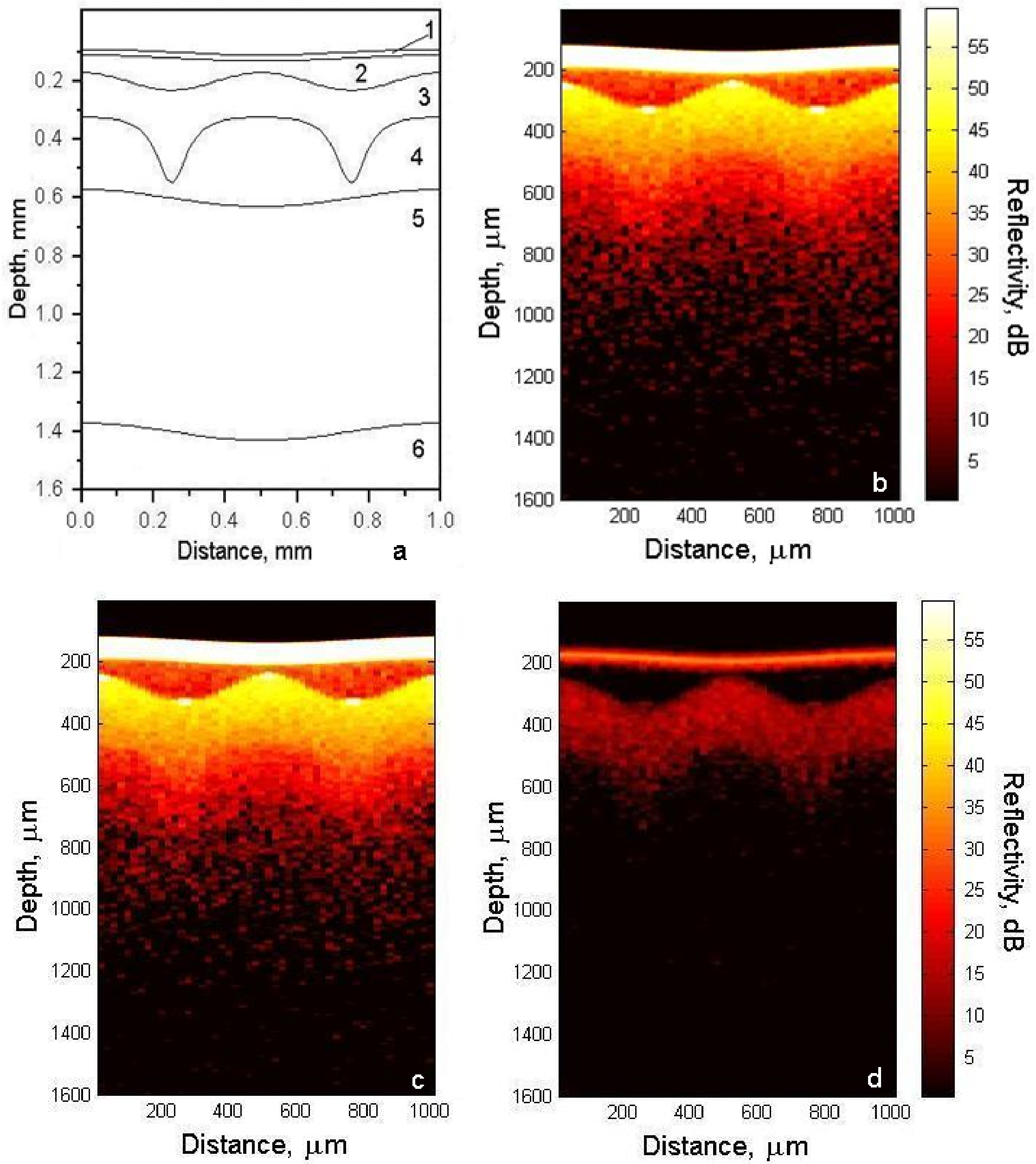

Meglinski, et al, *Optics Letters* (2008)

PS OCT Images Experiment

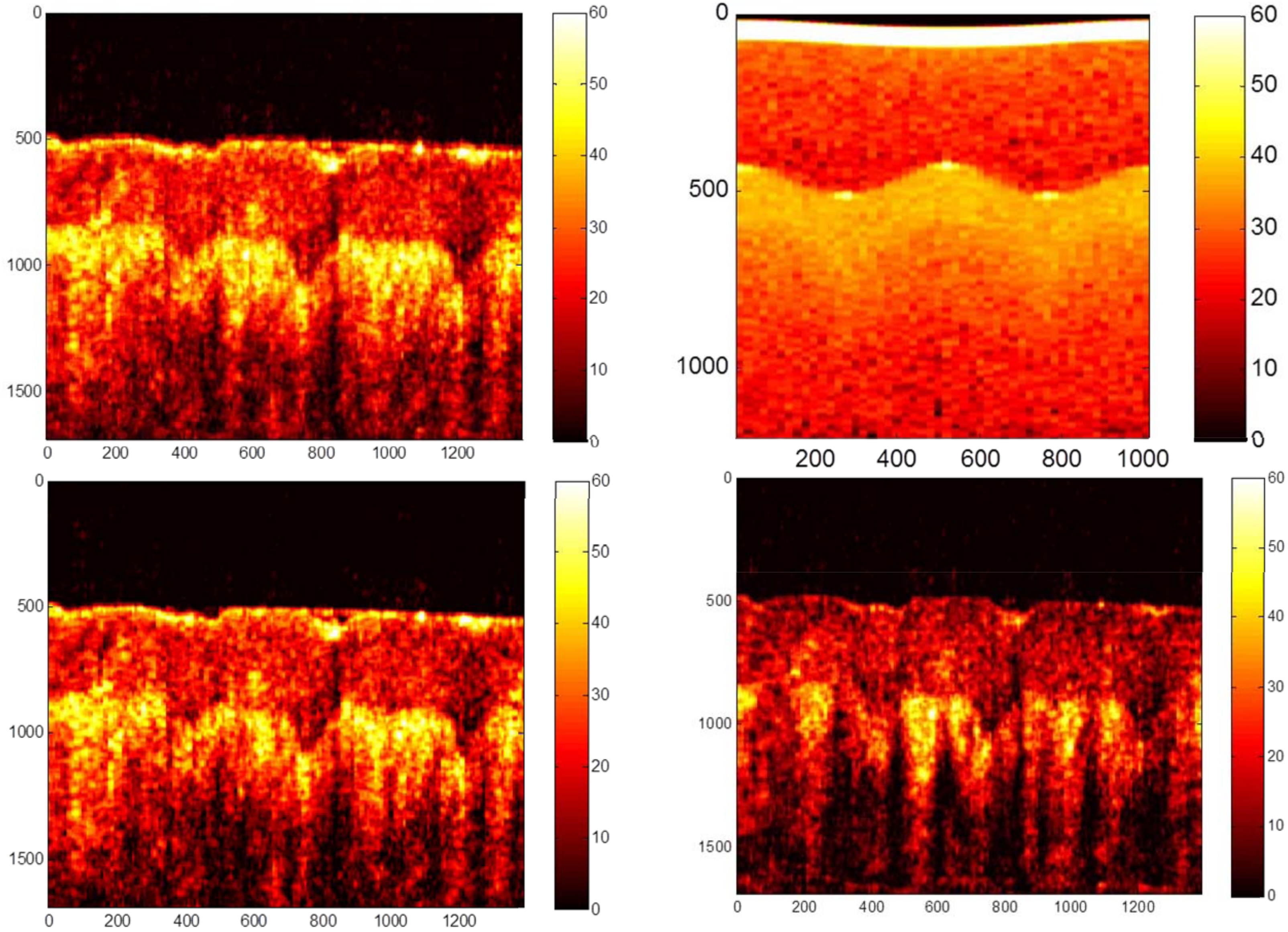

OCT images of skin for various coherence lengths: 3, 5, 15, 30 microns

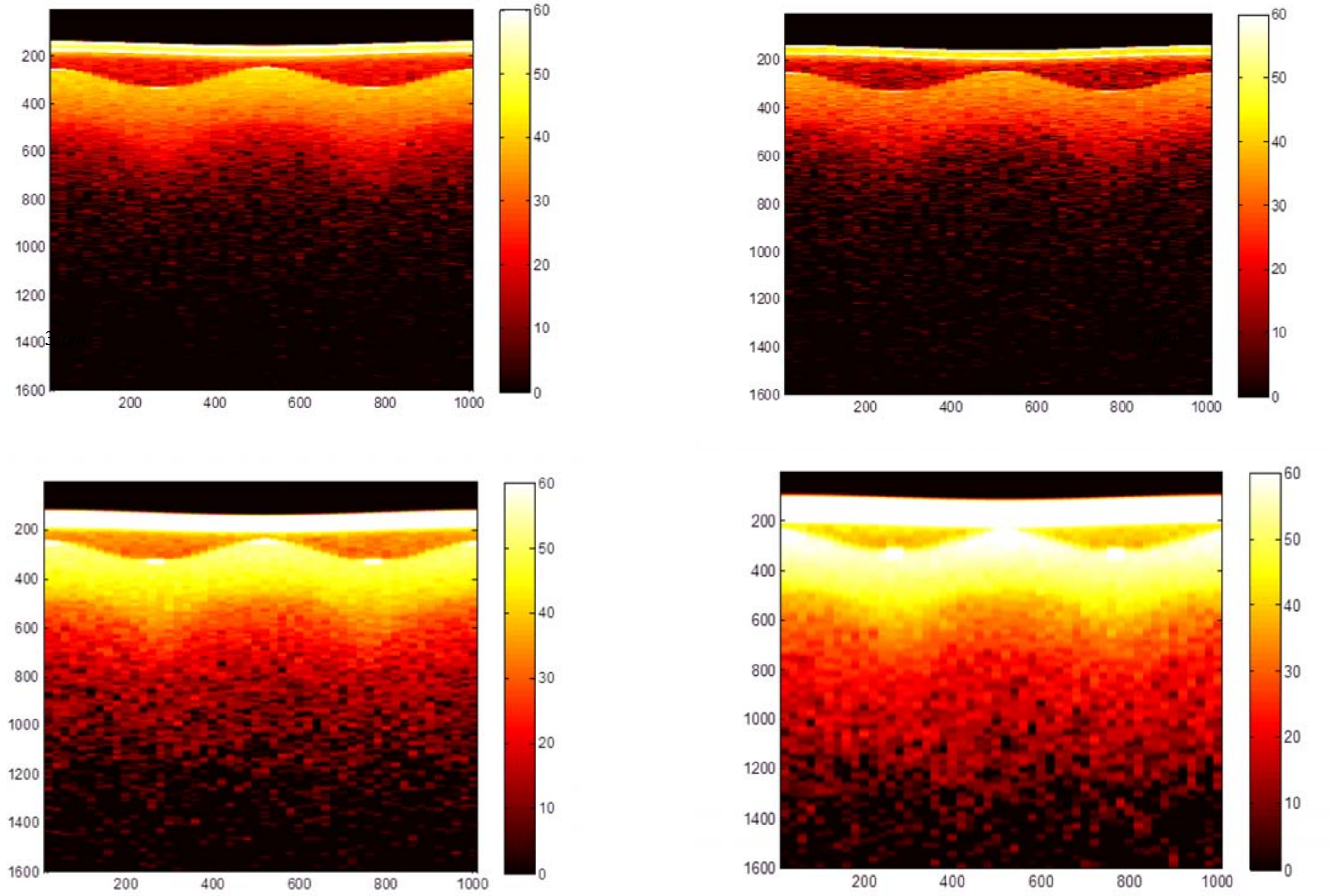

OCT Images Simulation - Speckles

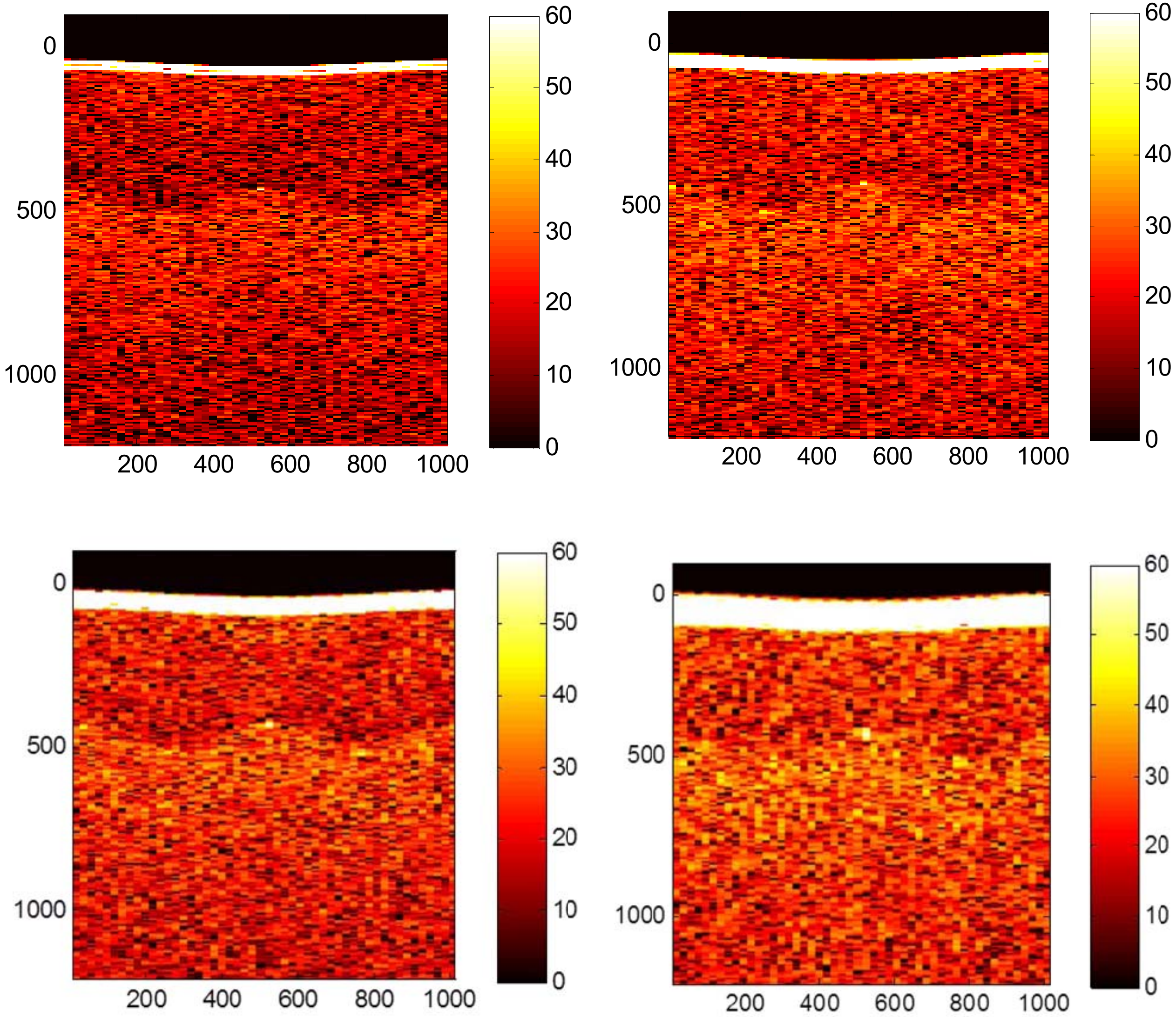

PS OCT images

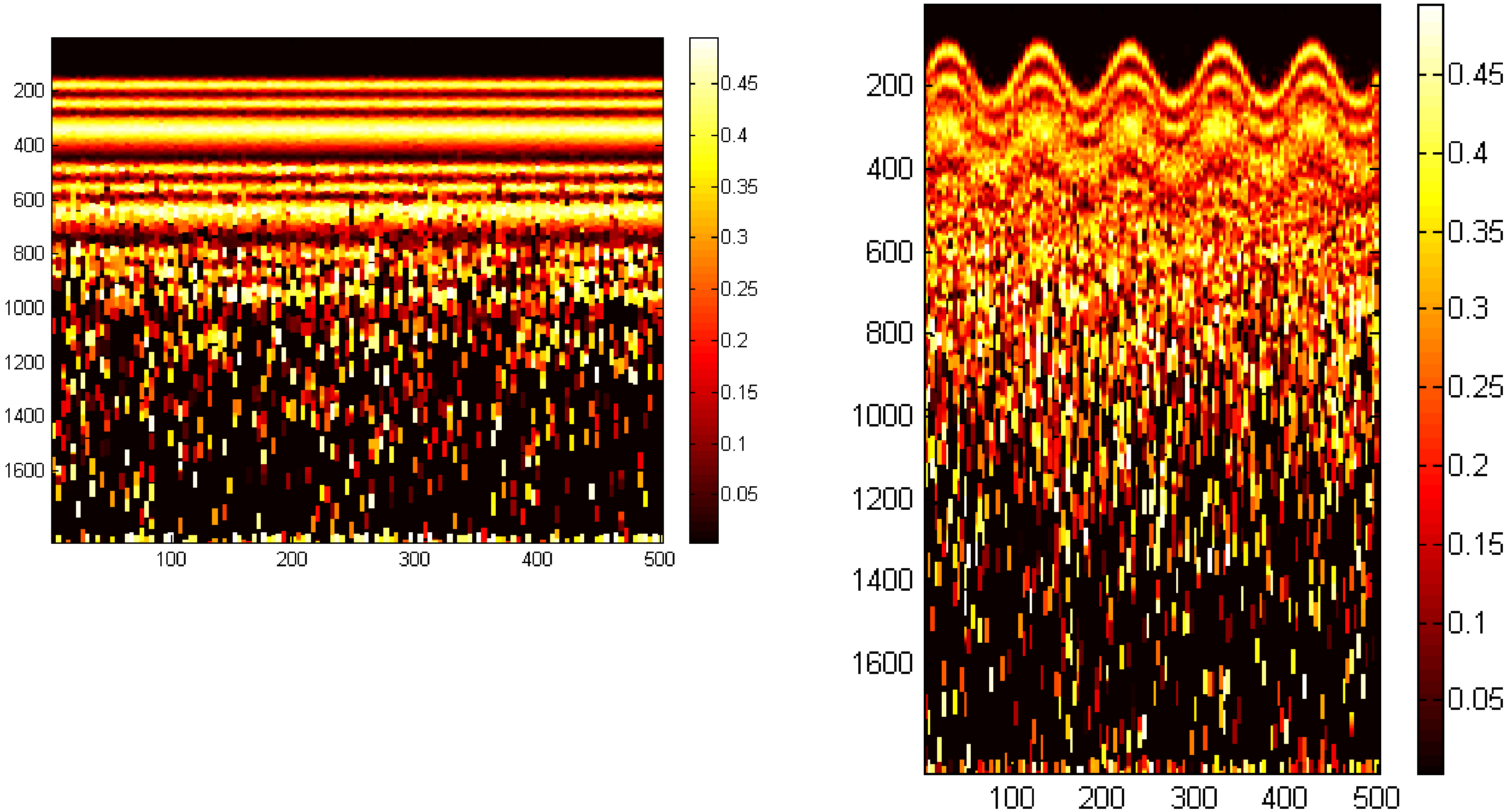

Phase retardation patterns for 12-layer birefringent media (tendon model): a – plane layers, b – non-plane layers

Summary

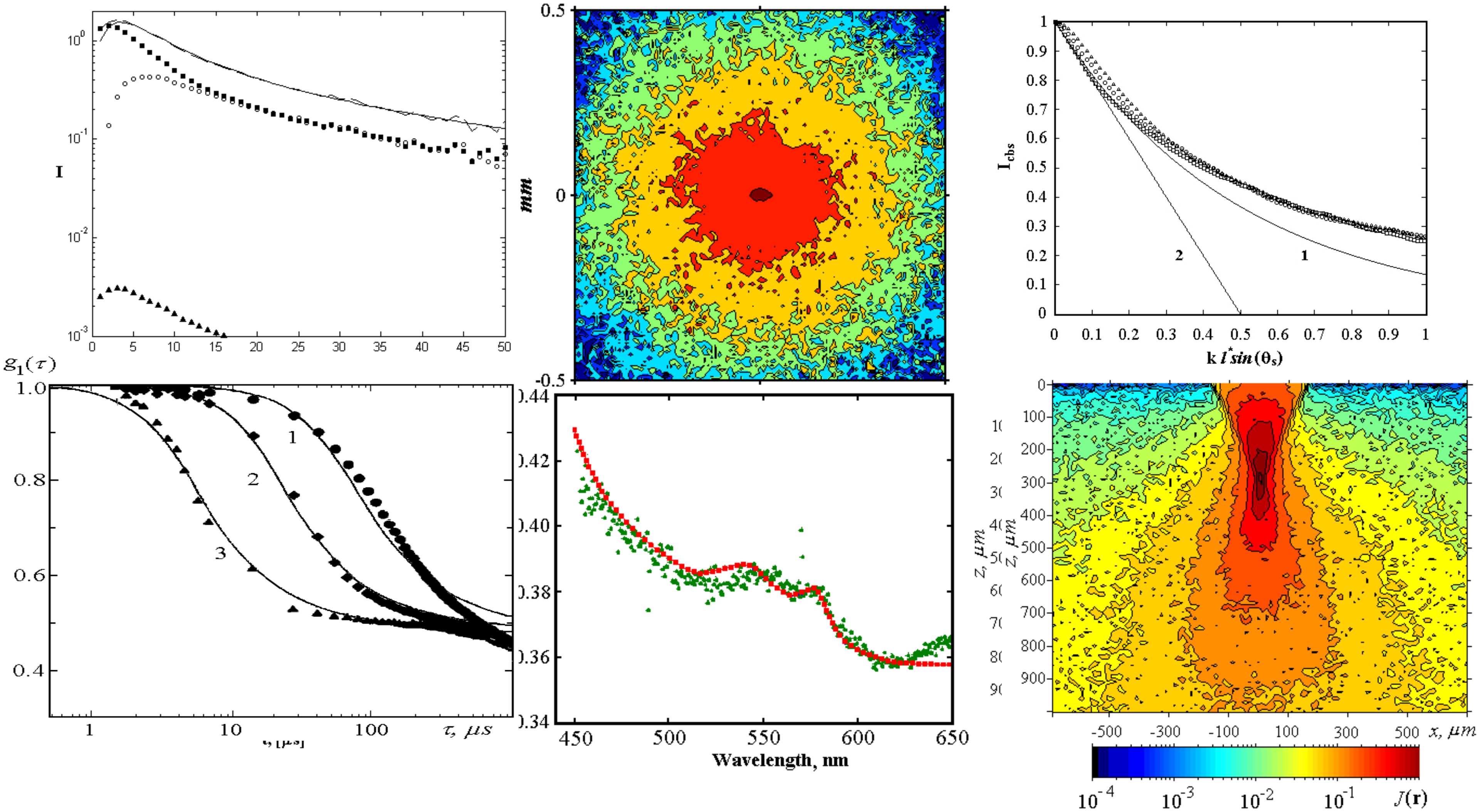
I
$g_1(\tau)$
τ, μs
1
2
3
mm
Wavelength, nm
I_{cbs}
$k\, l^* sin(\theta_s)$
1
2
z, μm
x, μm
$J(\mathbf{r})$

Acknowledgements

EPSRC and BBSRC, UK
The Royal Society, UK
The Royal Academy of Engineering, UK
NATO
LaserLab, Europe
European Commission, EU
CRDF, USA
and
British Council, UK